REGOLITH GEOLOGY AND SOIL GEOCHEMISTRY OF THE LITTLE EVA COPPER PROSPECT, QUAMBY DISTRICT, NW QUEENSLAND

Volume I

I.D.M. Robertson, C. Phang and T.J. Munday

CRC LEME OPEN FILE REPORT 123

April 2002

CRC LEME

CRC

REGOLITH GEOLOGY AND SOIL GEOCHEMISTRY OF THE LITTLE EVA COPPER PROSPECT, QUAMBY DISTRICT, NW QUEENSLAND

Volume 1

I.D.M. Robertson, C. Phang and T.J. Munday

CRC LEME OPEN FILE REPORT 123

April 2002

© CSIRO

CSIRO/CRC LEME/AMIRA PROJECT P417
GEOCHEMICAL EXPLORATION IN REGOLITH-DOMINATED TERRAIN, NORTH QUEENSLAND 1994-1997

FRONTISPIECE

Air photograph of the Little Eva Prospect, showing the erosional regime (ER) in blue-grey, the alluvial unit of the depositional regime (AL) in red-brown with Cabbage Tree Creek (CT), and the complex colluvial units (CO) in yellow-brown. The ribbed pattern of cracking clay soils (CK) is clearly seen in the south-east. Final dismantling of the colluvium is taking place along a small creek (CX) which follows the patterns of the 'gilgai'. The prospecting trenches were open at the time of the photograph.

PREFACE AND EXECUTIVE SUMMARY

The principal objective of the P417 Project is to improve substantially geochemical methods of exploration for base metals and Au in areas obscured by weathering or under younger cover. The research includes geochemical dispersion studies, regolith mapping, regolith characterisation, dating of profiles and investigation of regolith evolution. Aspects of this report cover, to some extent, all of these, except for regolith dating. Specific objectives include a series of case studies. This is the first such case study to be completed.

The problem confronting exploration at Little Eva is the presence of a shallow mantle of colluvium masking prospective ground to the south of the Prospect and alluvium masking it to the north. In places black soil has developed within the colluvium. These problems are common throughout much of the Eastern Succession, where stony colluvium masks much of the ground between low ridges. Weathering of the basement rocks is not particularly intense and there is no lateritic duricrust or mottled zone material in evidence. Common practice, in these circumstances, is to resort to expensive bedrock sampling, involving drilling through the colluvium into a relatively lightly weathered material in which, from experience on the Yilgarn Craton, dispersion is likely to be minimal. This necessitates close-spaced drilling. If surficial sampling could be employed and natural dispersion used, exploration costs could be reduced substantially.

Copper and Au are the only indicator elements, from among 44 elements, which detect the Little Eva style of mineralisation in the soil. With careful interpretation, these depict the bedrock Cu anomaly beneath the colluvium. Iron, Co and V may be used to trace magnetite-rich rocks which may have exploration significance.

This case study has demonstrated the value of regolith and soil type mapping as an essential adjunct to planning a surficial geochemical survey and to its later interpretation. As this is the first P417 study in the district, conclusions on regolith evolution must be regarded as preliminary, particularly in view of the lack of sectional exposure. District-scale regolith mapping and regolith characterisation will continue to be used to establish the regional distribution of regolith types and to understand regolith evolution.

R.R. Anand
Project Leader

I.D.M. Robertson
Deputy Project Leader.

14th June 1995.

CONTENTS

10   REFERENCES   45

1   ABSTRACT

The Little Eva Cu Prospect is located 12 km north of the Dugald River Zn-Pb orebody and is situated in scapolitic granofelses of the Corella Formation and is associated with feldspar porphyry and magnetite-rich rocks. Although, in the vicinity of the Little Eva shaft, these rocks are exposed or occur under a very thin soil, the prospective rocks to the south are masked by colluvium. This prospect had been investigated intensively by CRA Exploration Pty Ltd., (CRAE), using the geochemistry of samples drilled from bedrock.

The geomorphology and regolith units were investigated on a district and on a local scale. This was to provide the setting for an orientation survey to test the effectiveness of soil sampling in areas where there is a thin layer of transported cover. South of the Little Eva Cu Prospect, detritus, from low quartzite hills and quartz veins, has been shed onto pediments gently inclined, towards Cabbage Tree Creek, to form a thin colluvial mantle of acid red earths with a quartz- and quartzite-rich lag. Near Cabbage Tree Creek, erosion has been active, etching into and through the colluvium, exposing the basement. This is largely covered by a thin, carbonate-rich lithosol, characterised by a lag rich in quartz and magnetite clasts. The magnetite is primary, although it has been partly weathered at the surface or near-surface. To the north, the area is dominated by alluvium and colluvium on which black clay soils are developed. Part of the colluvium, south of the Prospect, has been almost completely dismantled, leaving an area of linear 'gilgai', occupied by dark brown, smectitic, cracking clay soils.

Soil sampling on an approximately triangular 200 m grid, shows that Cu and Au are the only indicator elements for Little Eva style mineralisation. Muted anomalies in both elements indicate the trend of the bedrock Cu anomaly, as determined by CRAE, even through the thin colluvium. The fine fraction (<75 μm) is more effective than the coarse (710-2000 μm) fraction. Iron, Co and V in the soil indicate concentrations of magnetite which may have some exploration significance.

Bioturbation by ants and termites and/or hydromorphic dispersion could have contributed to moving the Cu and Au geochemical signal in the fine fraction upward from the basement and through the colluvium. However, the low tenor of the anomalies requires that careful attention be paid to setting the correct thresholds and the use of appropriate display methods (e.g., logarithmic scales).

2 INTRODUCTION

2.1 Location, access, climate and vegetation

Little Eva (Figure 1) is in the Quamby district, 12 km north of the Dugald River Pb-Zn-Ag deposit, about 90 km north-east of Mt Isa at 20° 8' 51"S, 140° 8' 39"E. Access is via CRAE's Dugald River camp, by exploration and farm tracks.

The Quamby district has a dry savanna climate (Blake, 1987). There is an average of 28 days per year with a maximum temperature above 40°C and the average annual rainfall is 450-500 mm, falling between November and March. Most of the area supports stunted eucalypts (3-8 m) some acacia scrub, scattered kurrajong trees and abundant spinifex and ephemeral grass species.

2.2 Objectives

Although some of the Proterozoic granofelses of the prospect are exposed, most are masked by shallow (1-2 m) colluvium and alluvium. The first objective was to map the regolith and characterise its component units, including the soil, both on a regional scale and locally around the Little Eva Cu Prospect. The second objective, was to determine whether soils could be used as a reliable geochemical sampling medium in areas masked by the colluvium and alluvium. If so, which are the most useful size fractions and which elements were the most effective indicators.

2.3 CSIRO work program

Research by CSIRO comprised studies of the surficial geology and the geomorphology followed by the geochemistry of soils developed from the weathering of the Proterozoic basement and in colluvium and alluvium. At the time of the study, the pits and costeans (frontispiece) around and south-west of the Little Eva shaft had been filled in.

3 REGIONAL AND LOCAL GEOLOGY

Little Eva lies in the Corella Formation of the Eastern succession of the Queensland Proterozoic. The oldest rocks lie east of the Mt Rosebee Fault and consist of amphibolite facies metasediments intruded by the Naraku Granite (1754 ± 25 ma; Wyborn et al., 1988). To the west of the fault, the metamorphic grade is greenschist facies and the rocks young to the west.

In the immediate environs of Little Eva, the succession (Edwards, 1979) from east to west is listed below with brief notes:-

Eastern metasediments
Well-laminated, flaggy, calcareous, micaceous and feldspathic, pelitic metasediments with thin, white and pink limestone interlayers.
Grey, micaceous and siliceous cap rocks over more calcareous units to the west.

Eastern carbonates
Interlayered scapolitic limestones with fine-grained, calcareous, feldspathic and micaceous, quartzose metasediments, including a cupriferous, podiform magnetite lens horizon.

Feldspar-silica caprocks developed over scapolitic limestone.

Cainozoic

☐ Colluvium

Mid Proterozoic

[+ + +] Granite

[∴∴∴] Knapdale quartzite

[////] Dugald River Depository

[o o] Other Proterozoic rocks

◜ Fault

Mt Isa Inlier

Little Eva

Barkly Hwy

Dugald River

Mt Isa

Cloncurry

Cannington

N.T. | Q.

138°   140°

-20°

-22°

0 ⊢——— 5 km

Little Eva Cu

Cabbage Tree Ck

Mt Rosebee Fault

Dugald River

Dugald River

to Cloncurry

20°20'

140°10'
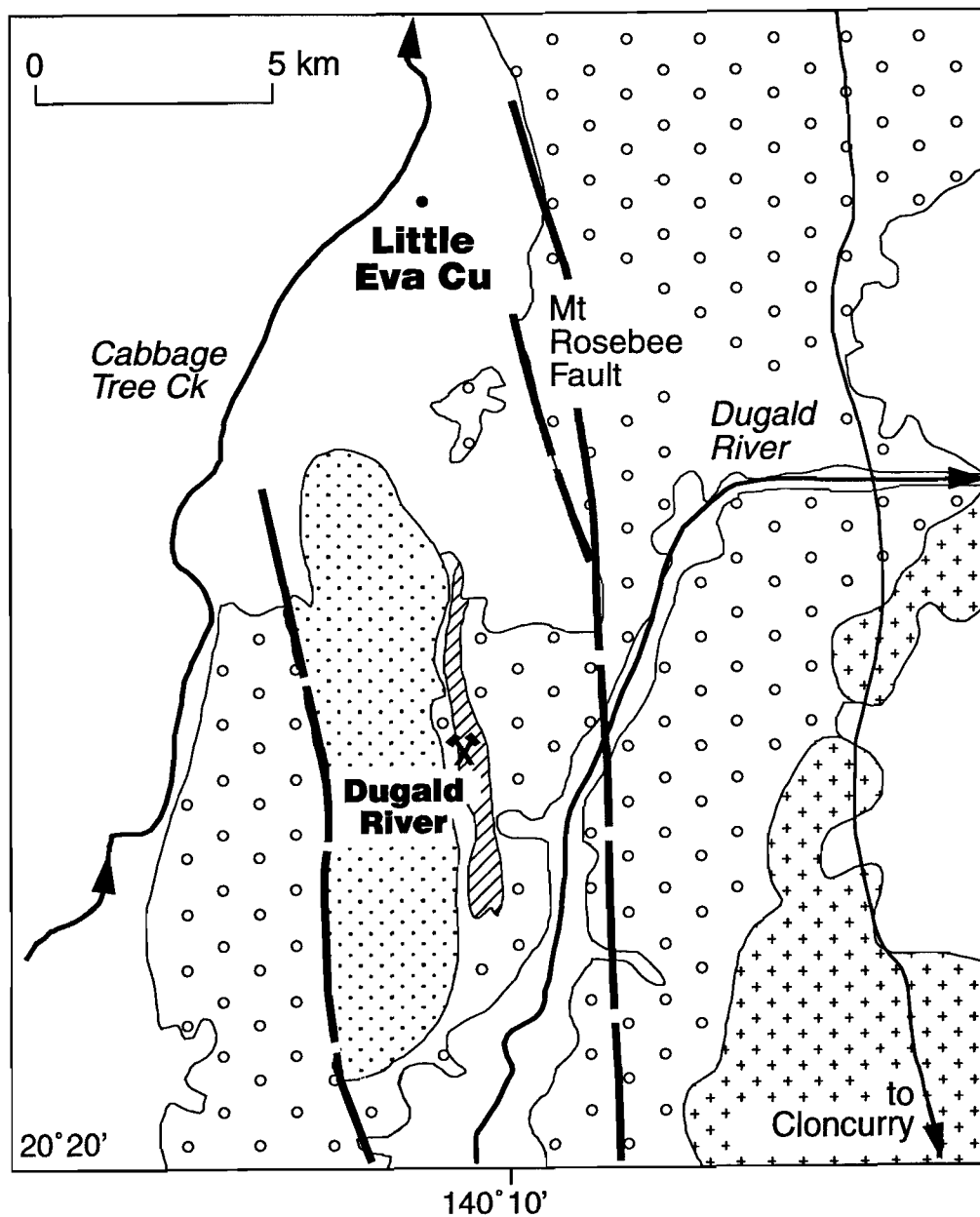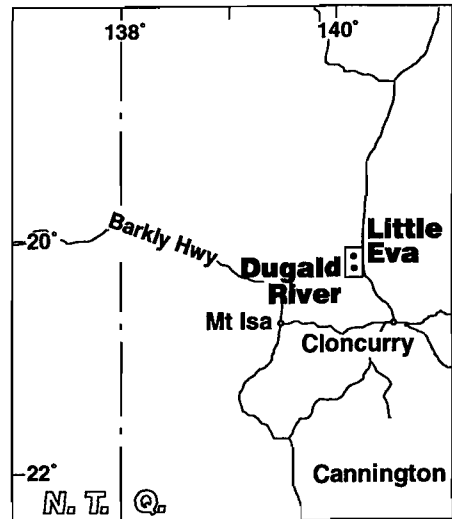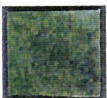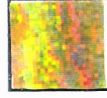
Figure 1. The geology around the Little Eva Cu Prospect, Queensland (after Wilson *et al.*, 1976).

Figure 2: Landsat TM Image - Map of regolith-landform units of the District about the Little Eva Prospect. The image (opposite) is a ratio colour composite comprising band ratios: 1.6/2.2 μm (Band 5/Band 7) - red, 0.83/2.2 μm (Band 4/Band 7) - green, and 0.83/0.56 μm (Band 4/Band 2) - blue.

Image Colour Pattern	Landform	Regolith Material
	Pediment and colluvial-alluvial plain	Red-brown to black clay soils, with some polymictic lag of ferruginous and other lithic fragments, including quartz.
	Pediment and colluvial-alluvial plain	Red-brown sands and silts, making up colluvial and alluvial sediments. Colluvial sediments generally covered by fine to medium polymictic lag, comprising lithic and quartz fragments.
	Pediment	Subcrop and outcrop with thin, red lithosols commonly covered by medium to coarse, blocky polymictic lag comprising lithic fragments (some ferruginous), quartz and nodules of pedogenic carbonate. Pedogenic carbonates are locally present.
	Pediment	Thin veneer of scattered colluvial sediments, comprising red-brown sandy soils, with fine-medium polymictic lag, over subcrop and outcrop.
	Low hills	Outcropping quartzites and quartz veins and ridges with coarse, blocky, quartz-rich lag and thin lithosols in places.
	Braided channels	Vegetation (white) over channel deposits.

Little Eva

Cabbage Tree Creek

Knapdale
Quartzites

Scale 1:60,000

N
△

0

2.5 km

Lode units

Massive granofels units, with transitional phases on contacts; principal units are:

      a) porphyroblastic scapolite-biotite granofels

      b) feldspar-chlorite-epidote-amphibole granofels

      c) feldspar porphyry.

Western carbonates

Interlayered scapolitic limestones with fine-grained, calcareous, feldspathic and micaceous, quartzose metasediments, including a podiform magnetite lens horizon. Red feldspar-silica caprocks, developed over scapolitic limestones.

Most of the Proterozoic rocks around Little Eva are obscured by extensive gravel plains on colluvium-alluvium, containing subangular to rounded quartzite clasts, a sandy alluvium in the vicinity of Cabbage Tree Creek and, where the basement rocks subcrop, thin, skeletal soils. The thickness of the alluvium is estimated at about three to five metres; the colluvium is probably very thin, generally one to two metres. Cabbage Tree Creek has incised to Proterozoic basement rocks in its bed; also relatively fresh bedrock is exposed close to the lower contact of the colluvium, where small streams have incised the regolith.

4   REGOLITH-LANDFORM RELATIONSHIPS

4.1   District regolith-landform setting

Regional variations in regolith material are well illustrated by a Landsat TM ratio colour composite image (Figure 2). The band ratios are those used for discriminating between different regolith-landform units in other deeply weathered terrains (Gozzard *et al.*, 1992) in the northern Yilgarn Craton. The image shows the spatial variation of the units but, because the spectral bands are broad, certain regolith-landform associations are combined. This is particularly true where materials have similar mineralogies and, therefore, similar spectral characteristics. Nevertheless, the image effectively defines patterns of regolith materials and shows their variability.

The Little Eva prospect is situated near to the confluence of two braided channel systems that drain the eastern and western sides of the Knapdale Quartzite - a ridge of low hills lying due south of the area. The prospect is sited on a gently inclined, undulating pediment which is covered by a veneer of thin, colluvial sediments and ferruginous lithosols. A medium to coarse polymictic lag, consisting of ferruginous and non-ferruginous, lithic fragments, with quartz and scattered nodules of pedogenic carbonate, is characteristic of the mineralised area, particularly in areas where bedrock outcrops.

In the NW portion of the Landsat TM scene, the area is dominated by colluvial-alluvial materials (blue) with extensive 'blankets' of black clay soils (drab olive-green) developed over them. On the eastern side of Cabbage Tree Creek, the cover of colluvial and alluvial material is thinner and more patchy. The pediment flanking the north and east of the Knapdale quartzites (yellow-green) is mantled by acid red earths and a lag of coarse to medium grained ferruginous gravel, lithic fragments and quartz (blue). This cover is less well developed to the east and south-east of Little Eva, where ferruginous lithosols (orange-green) are common on the flanks of small gullies and creeks, with colluvial materials generally on the crests of the interfluves. Erosion is active in these areas. Small patches of gilgai - black clay soils - have developed in some of these areas. Quartz float, where it forms a dominant component of the surface lag, appears yellow on the image.

Legend:

- Alluvium
- Colluvium
- Colluvium with "gilgai"
- Proterozoic basement
- • Soil samples

Map labels:

11500mE   12000mE

Cattle pen

Cabbage Tree Creek

Little Eva
X

26000mN

25500mN
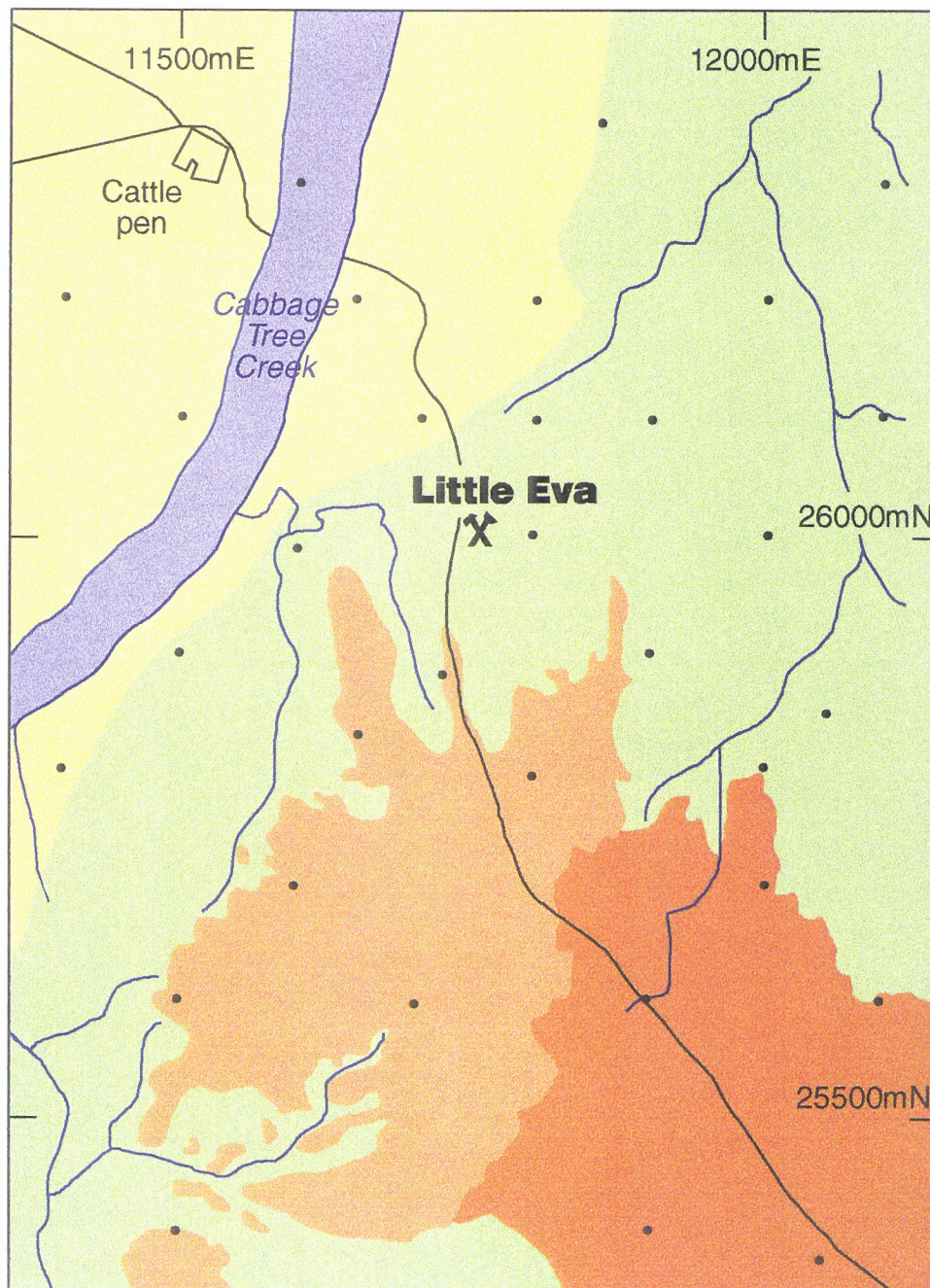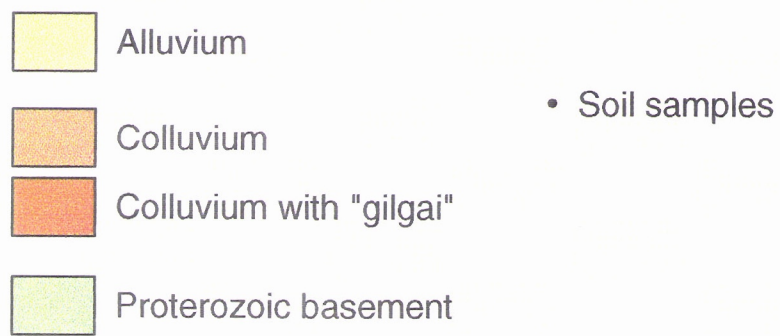
Figure 3. Regolith map of the Little Eva prospect.

FIGURE 4

DETAILS OF FIELD EXPOSURES

A. Detail of the lag exposed on the lithosol covering eroded Proterozoic basement. Angular vein quartz (QZ), subrounded quartzite clasts (QT) and round magnetite clasts (MT) on a very pale brown, carbonate-rich soil. Location 26050N, 11900E.

B. Termitaria (TM) on a thin veneer of colluvium (CO). The eroded basement occupies the slightly lower ground in the background (ER). Location approximately 25900N, 11900E.

C. Angular quartz (QZ) and subangular brown quartzite (QT) lag on a brown, carbonate-free soil (SO) overlying colluvium. Note the absence of magnetite 'nodules'. Location approximately 25950N, 11900E.

D. A lag of white quartz (QZ) and more abundant brown quartzite (QT) overlying colluvium in the southern part of the area. Note the presence of abundant magnetite clasts (MT). This lag type is interspersed with brown 'gilgai' soils. Location approximately 25600N, 12000E

E. Slightly elevated areas of red-brown soil with quartz and quartzite lag (BZ), interspersed with a slightly lower, linear tract of lag-free, darker brown cracking soil (CK). Note the development of grasses on the cracking soils contrasted with spinifex, bushes and small eucalypts on the lag-covered areas. Location approximately 25500N, 11850E.

F. The brown soil of a 'gilgai'. Note the deep cracks (CX) in the soil substrate and the grass cover. Location approximately 25650N, 11820E.

G. The uncracked brown fine soil on the alluvium. Location 26014N, 11580E.

H. A small, pod-like outcrop of magnetite (MT). These and smaller outcrops and subcrops shed a copious lag onto the soils on the eroded Proterozoic basement and are probably quite common in the environs of the Little Eva mineralisation. Location approximately 25650N, 11380E.

Figure 4

11
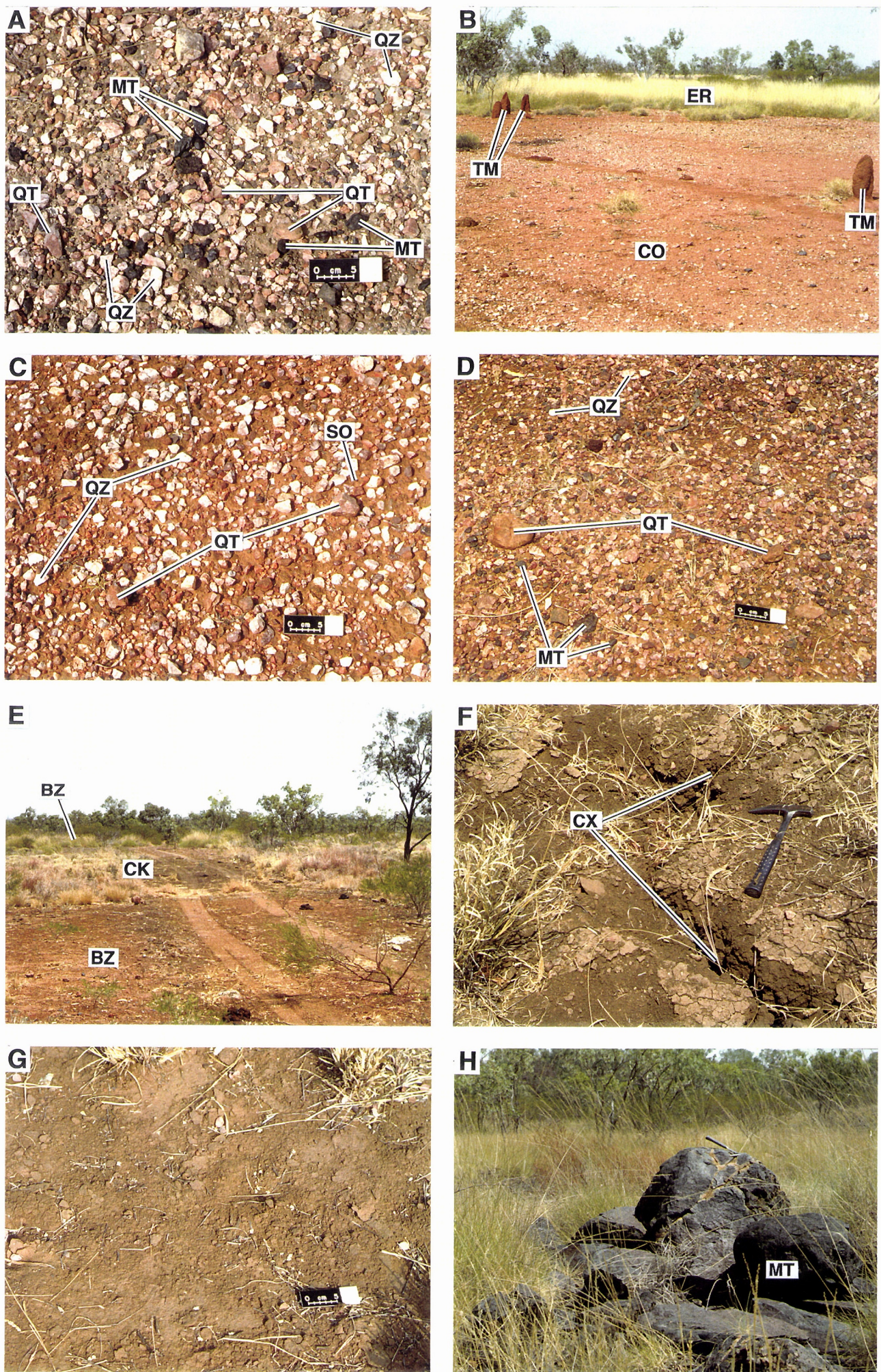
4.2 Local regolith-landform setting

Detailed regolith mapping (Figure 3) around the Little Eva Prospect shows two main regolith regimes, erosional and depositional; the depositional regime may be subdivided into one alluvial and two colluvial units. Soils at each sample site are described in Appendix 4.

4.2.1 Erosional regime

In the immediate vicinity of the Little Eva Prospect, the colluvium has been partly eroded. Here, very low outcrops of fresh Proterozoic bedrock of the Corella Formation and its saprolite are partly mantled by a skeletal, grey soil, rich in lithic fragments. It is overlain by a lag of white quartz, pinkish quartzite and numerous subrounded magnetite fragments (Figure 4A). This erosional regime extends south-west, in a narrow strip, along the eastern flank of Cabbage Tree Creek and has been incised weakly by small streams. It is covered with grassland interspersed with small eucalypts. To the north and east, the Proterozoic rocks have been more intensely eroded into gently undulating country with a grey-blue airphoto tone, characterised by surface carbonates.

4.2.2 Depositional regimes

The depositional regimes, consist of an alluvial unit, north of the eroded basement, and two colluvial units to the south.

Colluvial Units

To the south-east, the Proterozoic rocks are hidden by a very thin veneer of transported colluvial material occupying a low plateau. The colluvium may be subdivided into two units. One, in the south-central part of the mapped area, is marked by spinifex with sparse trees, a yellowish tone on the air-photos and is characterised by tall, red-brown termitaria (Figure 4B). It is mantled by a lag, rich in angular to subrounded quartzite clasts, round quartzite cobbles, a few fragments of vein quartz and very minor, rounded magnetite pebbles set in a red-brown, lithic, carbonate-free soil (Figure 4C). This material appears to occupy very slightly higher parts of the landscape than the colluvium-covered area to the southeast.

The other subdivision of the colluvium occupies the south-east part of the mapped area. There are fewer trees and this unit is characterised by numerous, elongated shallow, grassy depressions (gilgai), underlain by grey-brown clays with a coarse cracking pattern (Figure 4F), interspersed with slightly elevated areas underlain by a yellowish colluvium and rimmed by spinifex (Figure 4E). The areas of self-mulching, cracking clays are elongate but, together, show a pattern reminiscent of drainage or pondage in a very flat area, where they form a complex of linear rises, interspersed with linear depressed floors. These may represent a subdued drainage system, developed in the last stages of dismantling of the colluvium. Later and more advanced stages are seen in incised drainages on the flanks of this unit (frontispiece). Thus, the 'gilgai' may represent incipient stripping of the colluvium, leaving a very thin layer on the substrate. A lag of quartzite fragments and cobbles, vein quartz and slightly more common, rounded magnetite clasts occur on a red-brown, lithic soil (Figure 4D) but not on the cracking clays. In places, small outcrops of fresh, Proterozoic basement (carbonate rocks with calc-silicate minerals and malachite) within the 'gilgai' indicate that the cracking clays form a very thin cover.

The very coarse lags, mantling much of both types of colluvium, contrast with the relatively fine soils which underlie them, indicating either an exogenous origin for the lag or considerable concentration of the lag by removal of fine material; the former is the more probable.
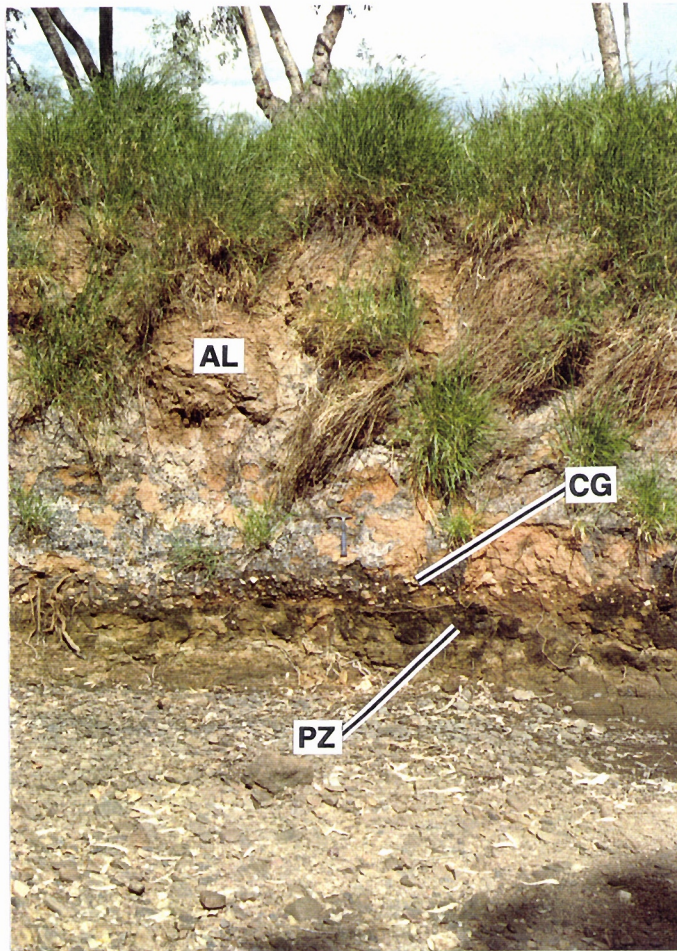
Figure 5. The base of the alluvium (AL) on deeply-weathered Proterozoic basement (PZ), overlain by a thin conglomerate (CG). Exposure in Cabbage Tree Creek. Location approximately 26050N, 11550E

FIGURE 6

PHOTOMICROGRAPHS

A. Coarse fraction (710-2000 μm) of a lithosol overlying the eroded Proterozoic basement. Subangular grains of granoblastic quartz (QZ) and a complex grain of relatively fresh granofels (GF), consisting of relatively fresh quartz, feldspar, epidote, magnetite and biotite. Transmitted light. Crossed polarizers. Specimen LE17B. Location 25900N, 11500E.

B. 75-250 μm fraction of a lithosol overlying the eroded Proterozoic basement. A polymictic material of separate grains of angular to subangular quartz (QZ), biotite (BI), hornblende (HB), magnetite (MT) and small granofels fragments (GF) consisting of quartz, feldspar, biotite, magnetite and hornblende. Transmitted light. Partly crossed polarizers. Specimen LE17E. Location 25900N, 11500E.

C. 75-210 μm fraction of a lithosol overlying the Proterozoic basement containing angular to subangular particles of quartz (QZ), epidote (EP), biotite (BI), brown, turbid plagioclase (PL) and granofels (GF) particles. Transmitted light. Partly crossed polarizers. Specimen LE17E. Location 25900N, 11500E.

D. 710-2000 μm fraction of a soil on the colluvium containing rounded to subrounded internally complex metamorphic rock (CX) and quartz (QZ) particles with well-developed weathered rims (RM) and cracks filled with Fe oxides (FX). Transmitted plain polarized light. Specimen LE23B. Location 25830N, 11650E.

E. 250-500 μm fraction of alluvium consisting of rounded to angular grains of quartz (QZ), clear microcline (MC), turbid plagioclase (PL), hornblende (HB), epidote (EP) and magnetite (MT). Transmitted light. Partly crossed polarizers. Specimen LE8D. Location 26100N, 11500E.

F. The internal structure of a round fragment of weathered magnetite (MT) from the soil of the erosional regime, showing octahedral spinel crystal form against quartz gangue (QZ). The magnetite is pitted and has been partly altered to kenomagnetite. Plain polarized reflected light.

G. The internal structure of a round fragment of weathered magnetite from the soil of the erosional regime, showing extensive alteration of (white) magnetite to (pinkish-grey) kenomagnetite. Plain polarized reflected light.

H. The internal structure of a round fragment of weathered magnetite from the soil of the erosional regime, showing the trellis structure of a spinel. Reflected light, crossed polarizers.

14

Figure 6

15
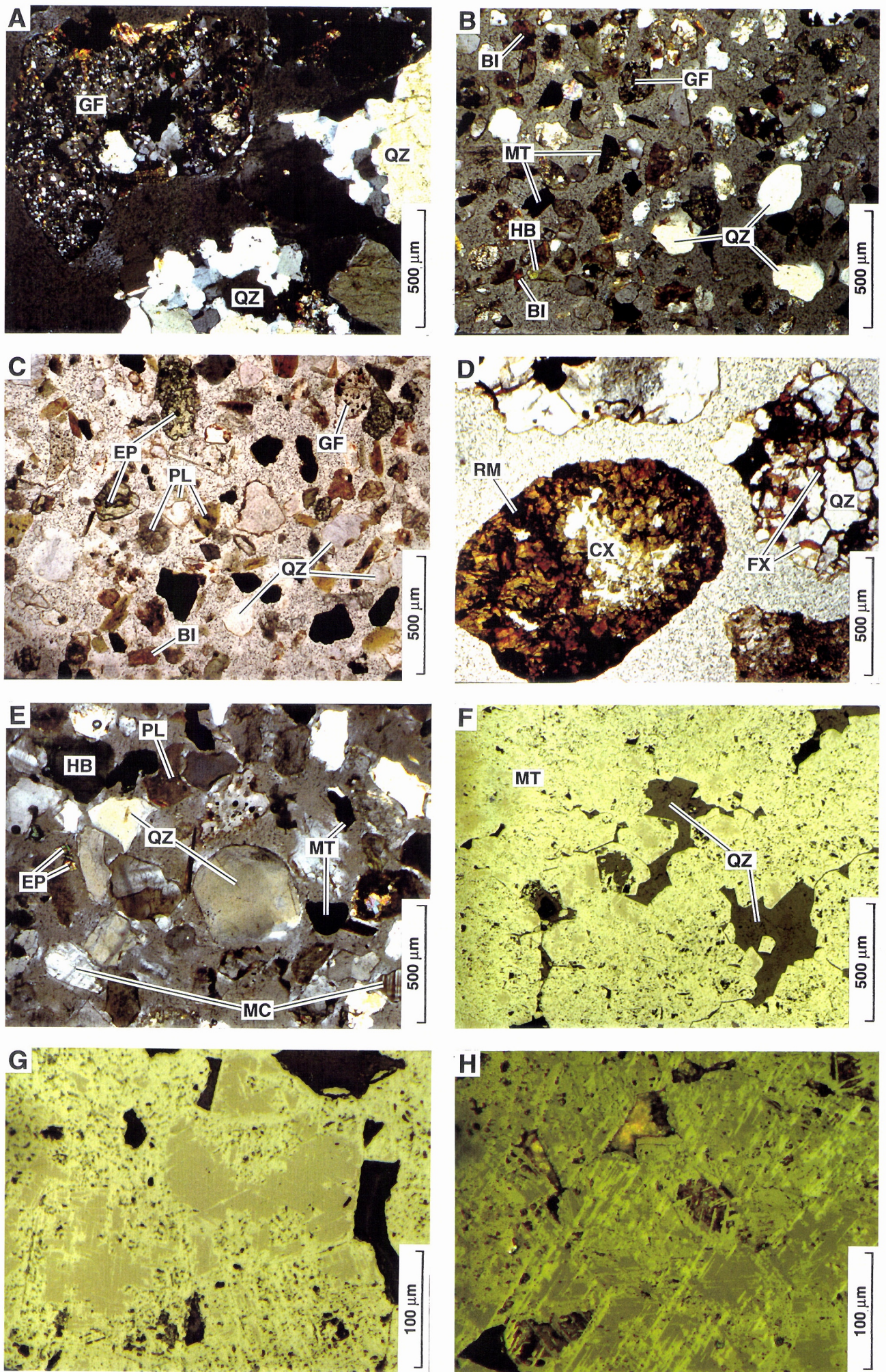
Alluvial Unit

The area to the north-west, flanking Cabbage Tree Creek, is blanketed by grey-brown to red-brown alluvium (Figure 4G), with a yellowish-brown photo-tone. The southeast boundary with the adjoining erosional regime is relatively linear, suggesting infilling of alluvial sediments against a small fault scarp. The bed of Cabbage Tree Creek has been graded slightly below the weathered Proterozoic basement (Figure 5). There is a thin (0.2 m) basal conglomerate, of subangular to round clasts, overlying saprolite, overlain by flood-plain sands and silts.

4.3   Magnetite pods

A number of small pods of magnetite outcrop in basement, both in the study area and outside it. Probably the largest occurs about 100 m south of a gate, a short distance south-east of the mapped area, where it forms a small hill, surrounded by a copious lag of black magnetite fragments on a red-brown soil. Close to the western margin of the mapped area, a small magnetite pod forms an outcrop in the erosional regime at about 11380E 25650N, and has shed a lag of black magnetite fragments (Figure 4H).

These pods are not weathering products as such but consist of lenses of slightly weathered 'primary' magnetite. In polished section, the opaque material shows both the outward form of magnetite, octahedral crystal faces which abut gangue materials (Figure 6F), and its internal trellis structure (Figures 6G and H). However, much of this material is now pinkish-grey kenomagnetite[1]. This initial oxidation is probably the effect of lengthy exposure in the zone of weathering.

Although the lag fragments, shed from the magnetite pods, are rounded, they should not be confused with lateritic materials such as laterite nodules and pisoliths. They have no cutans and careful examination of their worn surfaces shows small crystal faces; this is more apparent on a freshly broken surface which also reveals quartz gangue, a highly variable magnetite grain size and reddish, earthy patches, where oxidation is advanced.

Variable quantities of magnetite lag are common in the soil of the erosional regime and in their derived lag. Lesser quantities of this material occur in some soil and lag overlying the colluvium. Either these materials have been carried into the colluvium from far afield, suggesting that this material is quite widespread, or they have been moved vertically from the basement, through a thin colluvium, by bioturbation.

5   STUDY METHODS

5.1   Soil sampling

Soil samples were collected on an approximately triangular grid, using a sample spacing of 150-200 m. At each point on the grid, a suitable sample site was selected, as free as possible from contamination by drilling or from vehicle tracks. Co-ordinates were determined from the local grid peg system and notes were taken on the sample site environment, geomorphology and soil type. The top 50 mm of soil was scraped away over about 0.25 m^2 to remove any possible

---

[1] Kenomagnetite is not a recognised mineral name but a petrographic term for a partly oxidised form of magnetite, between magnetite and maghemite, with the formula $Fe_{3-x} Fe_x O_4$ where x is small and the second Fe atom is in the ferric state. Kenomagnetite, once formed, may remain largely unaltered, may oxidise to maghemite, invert to hematite or hydrate to goethite (Morris, 1985).

contamination. About 1 kg of complete soil was collected from a depth of 50-200 mm. Thirty-five soil samples were collected to represent a grid covering 1040 x 680 m (0.707 km^2).

5.2 Sample preparation

Five sub-samples, from soils which represent different geomorphological environments (namely; erosional, and the two depositional), were selected for pilot treatment. They were wet sieved in deionised water into their principal components (>2000, 710-2000, 500-710, 250-500, 75-250, <75 μm), using nylon sieves in PVC supports and the sieved components were oven dried at 70°C. Each size fraction was weighed to determine its relative abundance and, hence, the practicality for later batch treatment. Specimens of each size fraction were reserved for microscopic examination. A selection from the >2000, 710-2000, 250-500 and <75 μm fractions were pulped and analysed. The results were assessed as a guide to later treatment of the complete batch.

Magnetite concentrates from fine soil material were obtained by wet sieving two selected Fe-rich soil samples to <75 μm and wet magnetic separation, using a 'Sepor' automagnet. The resultant magnetite-rich concentrate was refined three times before drying and XRF geochemical analysis. Subsamples of the remaining soil samples of the batch were wet sieved with brushing in deionised water and only the 710-2000 and the <75 μm fractions were oven dried at 70°C and pulped for analysis. Aliquots of 100 g or less of each sample was pulped using a K1045 steel mill. The mill was cleaned by quartz sand wash and alcohol wipe of the mill components between samples.

5.3 Petrography

Samples of the coarse (2000-710 μm) and fine (>75 μm) soil fractions were mounted in resin and separately sectioned and polished. These specimens were examined in oblique, reflected and transmitted light. Details of the mineralogy, fabric and the state of weathering of the soil particles were recorded.

5.4 XRD mineralogy

Pulped samples were examined by CuKα radiation, using a Philips PW1050 diffractometer, fitted with a graphite crystal diffracted beam monochromator. Each sample was scanned over a range 3-65° 2θ at a speed of 1° 2θ/min and data were collected at 0.02° 2θ intervals. Charts, plotted at 0.5° 2θ/cm were used for interpretation. Estimates of the abundance of specific minerals in different samples were made by measuring XRD peak heights in cm; this method does not take into account mass absorption, crystallinity etc., is very approximate and must not be used to compare the relative abundances of *different* minerals. The mineralogy of selected grains was determined by Debye-Scherrer diffractograms.

5.5 Chemical analysis

The pilot samples were analysed by XRF (CSIRO), by INAA (Becquerel Laboratories) and by ICPMS (Analabs). The batch samples were analysed by XRF and INAA only.

INAA
Aliquots of 10 or 30 g (depending on availability) were encapsulated at CSIRO and sent to Becquerel Laboratories for INAA analysis. Detection limits were as follows (in ppm):- K (2000); Fe (500); Zn, Ba, Na (100); Rb (20); Ag, Se, Cr, Mo (5); W, Ce, Br, U (2); As, Co, Cs, Ta (1); La, Eu, Yb, Hf, Th (0.5); Sb, Sm, Lu (0.2); Sc (0.1); Ir (0.02); Au (0.005).

XRF

X-ray fluorescence analysis was performed at CSIRO on fused discs (0.7 g sample and 6.4 g Li borate) using a Philips PW1480 instrument by the method of Norrish and Hutton (1969). Detection limits were as follows (in ppm):- Si, Al (100); Mg, Na (100); Fe (50); Ti (30); Mn, P (20); Ca, K (10); Ba (30); Ce, Cl (20); Cr, Co, Cu, La, Ni, S (10); Pb, Rb, Sr, V, Y, Zn, Zr (5); Nb (4); Ga (3).

ICPMS

ICPMS analysis was performed by Analabs (Perth). Prior to analysis, the samples were digested in $HNO_3/HCl/HClO_4/HF$ (Method GS201). Detection limits were as follows (in ppm):- Ag, Bi, Cd, Mo (0.1).

Data are presented in Appendices 1 and 2 and have been contoured in Appendix 3. Analyses of standards are presented in Appendix 5 and inter-element correlations in Appendix 6.

5.6 Data presentation

The data distribution in plan was just adequate for contouring (Appendix 3). The data for each fraction were gridded at a 25 x 25 m mesh, using a moving, weighted, least squares method (weighting exponent 2.0), utilising the nearest 8 points. The weighted values were used to compute a first order polynomial for each grid node. This method was chosen as it closely honours the control points. Minor difficulty was encountered with highly variable and skewed data (e.g., Cu) which, in the untransformed state, could produce contoured anomalies larger than that implied by point data. Log(10) transforms were applied and the data translated after contouring, to produce a more accurate and useful result. Linear contour plots of some skewed elements (e.g., Au), with much smaller ranges than Cu, lost some detail at low abundances; log(10) plots also improved the resultant spatial distribution patterns. Contours were smoothed using four filtering passes. Contour intervals were chosen to display the data with maximum sensitivity but minimum clutter. Similar contour intervals were applied to the course and to the fine fraction for each element where possible.

6   SOIL PHYSICAL ATTRIBUTES

6.1   Soil petrology

6.1.1   Eroded basement

Lithosols from the erosional regime contain much relatively unweathered material of the underlying lithologies, including amphibole, epidote, quartz, biotite and magnetite. They are rich in fragments of granofels saprock, angular quartz fragments, pieces of microcrystalline secondary carbonate (probably from calcrete which has penetrated the saprock), some coarse-grained primary carbonate (from carbonate veins and metamorphosed limestone pods) and variable quantities of magnetite nodules. These are all set in a fine-grained, dusty, generally carbonate-rich matrix.

Petrology of the 710-2000 μm soil fraction reveals a variety of slightly weathered to fresh fragments of granofels (Figure 6A with various metamorphic assemblages (e.g., quartz-magnetite-hornblende, quartz-epidote, quartz-carbonate-magnetite-hornblende, quartz-magnetite-chlorite, quartz-plagioclase-chlorite-magnetite, quartz-calcite-magnetite, calcite-magnetite-chlorite) there are also complex grains of vein quartz and coarse calcite. The plagioclase tends to

be weathered and is cloudy and brownish; fresh feldspars are largely microcline. Some calcite occurs as clear, coarsely-crystalline patches (primary, metamorphic); in others it is stained brown and microcrystalline and is probably secondary (calcrete and soil carbonate). Most of the magnetite is opaque and fresh, but some has been weathered to Fe oxy-hydroxides with locally stained grain boundaries. The quartz grains are angular and much of the material is of relatively fresh rock with minor saprock.

The 75-250 µm fraction (Figures 6B and C) consists mostly of separate, subangular mineral grains (quartz, magnetite, hornblende, carbonate, biotite, chlorite, epidote, and microcline) and a few fine-grained rock fragments. The plagioclase is turbid and there is a variety of carbonate crystallinity. The magnetite shows minor alteration to kenomagnetite.

Calcite is abundant in the east and, here, the majority of calcite grains are cryptocrystalline, with only a few coarsely crystalline grains (Sample LE-4c); others have a higher proportion of coarse calcite (Sample LE-12c).

6.1.2 Colluvium

The 710-2000 µm fraction of the soil on the colluvium consists of a variety of rounded to subrounded rock and mineral fragments, including vein quartz, microcline, and metamorphic assemblages (e.g., quartz-plagioclase-epidote, epidote-chlorite, quartz-magnetite-feldspar, quartz-muscovite, quartz-feldspar-hornblende) and igneous assemblages (e.g., plagioclase-altered pyroxene). Many of the rock fragments, particularly those rich in chlorite, are intensely stained by Fe oxides around their rims (Figure 6D). Quartz and quartzite grains also have stained rims and internal cracks are filled with Fe-oxides. Rounding of the grains, particularly those of quartz, staining and weathering of lithic fragments and the diversity of their origins (indicating metamorphic, granitic and volcanic provenances) suggest a significant transported component in the coarse material of the colluvium.

The 75-250 µm fraction consists of subangular to subrounded mineral grains, consisting largely of quartz and microcline with lesser amounts of magnetite, stained chlorite, epidote and hornblende. Many grains show an Fe oxide coating, a greater degree of rounding and a dominance of resistant minerals (quartz, K-feldspar, epidote) than those of the equivalent grain size in the erosional regime; this also implies a significant transported component. The magnetite of both colluvium fractions shows more extensive alteration to kenomagnetite, suggesting that magnetite in the colluvium has had a longer exposure to weathering.

6.1.3 Alluvium

The sandy fraction (710-2000 µm) indicates several provenances. Rounded, water-worn grains of quartz occur together with angular grains (Figure 6E), indicating varied transport distances. The dominance of rounded quartz and microcline grains suggest a large but distant granitic provenance but the less abundant but sharper epidote, magnetite and granofels fragments are probably more locally derived.

The 250-500 µm fraction consists of angular to subrounded mineral grains (quartz, k-feldspar, hornblende, epidote, magnetite, biotite, muscovite, turbid plagioclase) and a few fine-grained metamorphic rock fragments. The minerals are largely fresh and the magnetite shows little alteration to kenomagnetite, suggesting that the alluvial material was eroded from relatively unweathered terrain.
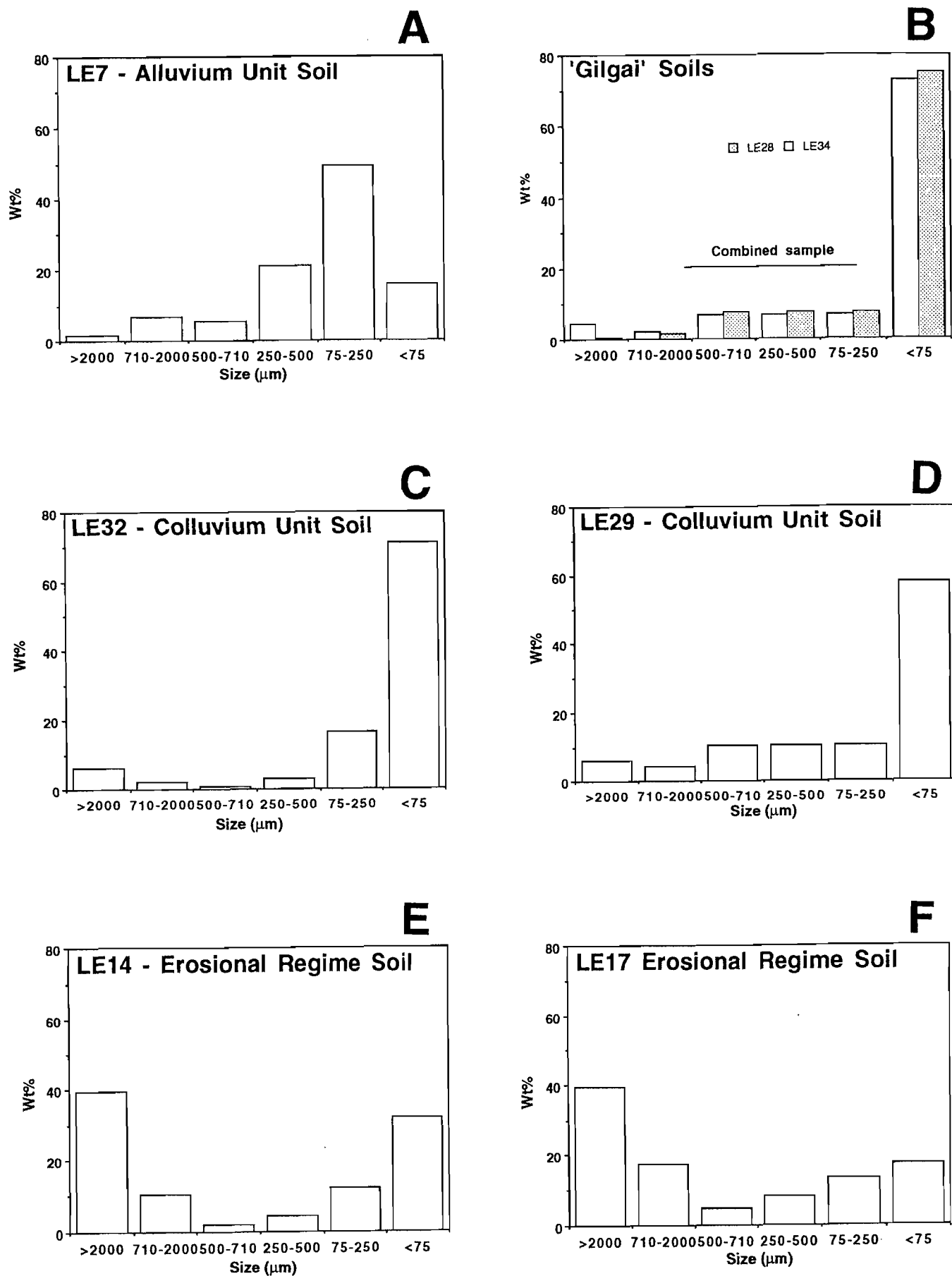
Figure 7. Size fraction analysis of samples from the erosional regime and from the colluvial and alluvial units of the depositional regime.

TABLE 2
RELATIVE MINERALOGICAL COMPOSITIONS OF SOILS

Sample	Environ	3.3 Quartz	3.0 Calcite	2.9 Dolomite	8.5 Amphibole	10.1 Mica	7.1 Kaolinite	14.3 Chlorite	15.0 Smectite	3.2 Feldspar	2.7 Hematite	2.5 Magnetite
LE23B	Coll	85.0	0.0	0.0	2.0	0.0	1.6	0.0	2.1	6.0	3.4	3.0
LE32B	Coll	90.1	37.4	0.5	0.0	0.0	0.4	0.0	0.0	13.6	0.4	0.0
LE14B	Ers	31.6	26.3	1.4	0.0	0.0	1.6	2.3	0.0	20.8	2.7	0.0
LE17B	Ers	53.4	31.8	4.3	0.0	1.2	0.5	2.4	0.0	14.5	3.1	0.0
LE06F	All	34.4	0.0	0.0	2.0	2.5	1.6	0.0	1.5	2.8	0.8	1.2
LE07F	All	32.3	0.0	0.0	2.7	4.0	1.8	0.0	0.0	6.8	2.0	1.0
LE23F	Coll	28.5	0.0	0.0	0.0	0.0	1.0	0.0	1.0	4.2	3.0	0.0
LE32F	Coll	67.3	0.0	0.6	1.3	0.0	0.8	0.0	4.5	2.1	1.3	0.0
LE28F	Coll(g)	52.4	0.0	0.0	0.0	0.0	0.5	0.0	2.5	4.0	1.0	0.5
LE34F	Coll(g)	64.8	0.0	0.0	0.7	0.0	0.5	0.0	4.5	4.0	0.6	1.2
LE04F	Ers	14.0	54.2	2.0	0.0	0.9	1.1	0.0	2.0	0.8	0.8	0.0
LE12F	Ers	39.4	29.6	1.0	1.0	2.0	0.8	0.0	4.0	0.0	4.5	0.5
LE14F	Ers	11.8	41.4	1.0	0.0	0.0	2.0	0.0	4.0	5.8	1.6	0.0
LE17F	Ers	17.3	40.0	4.5	0.0	0.5	2.0	0.0	3.0	2.2	1.5	0.0
LE18F	Ers	19.1	0.0	0.0	1.3	0.5	1.8	0.0	6.0	5.3	2.0	0.0

Samples labled 'B' are from the 710-2000 μm fraction
Samples labled 'F' are from the <75 μm fraction

Numbers refer to the XRD peak height in cm

Note: The numbers represent the XRD peak heights in cm; they
represent approximate differences between samples and should
not be used to compare abundances between different minerals

21
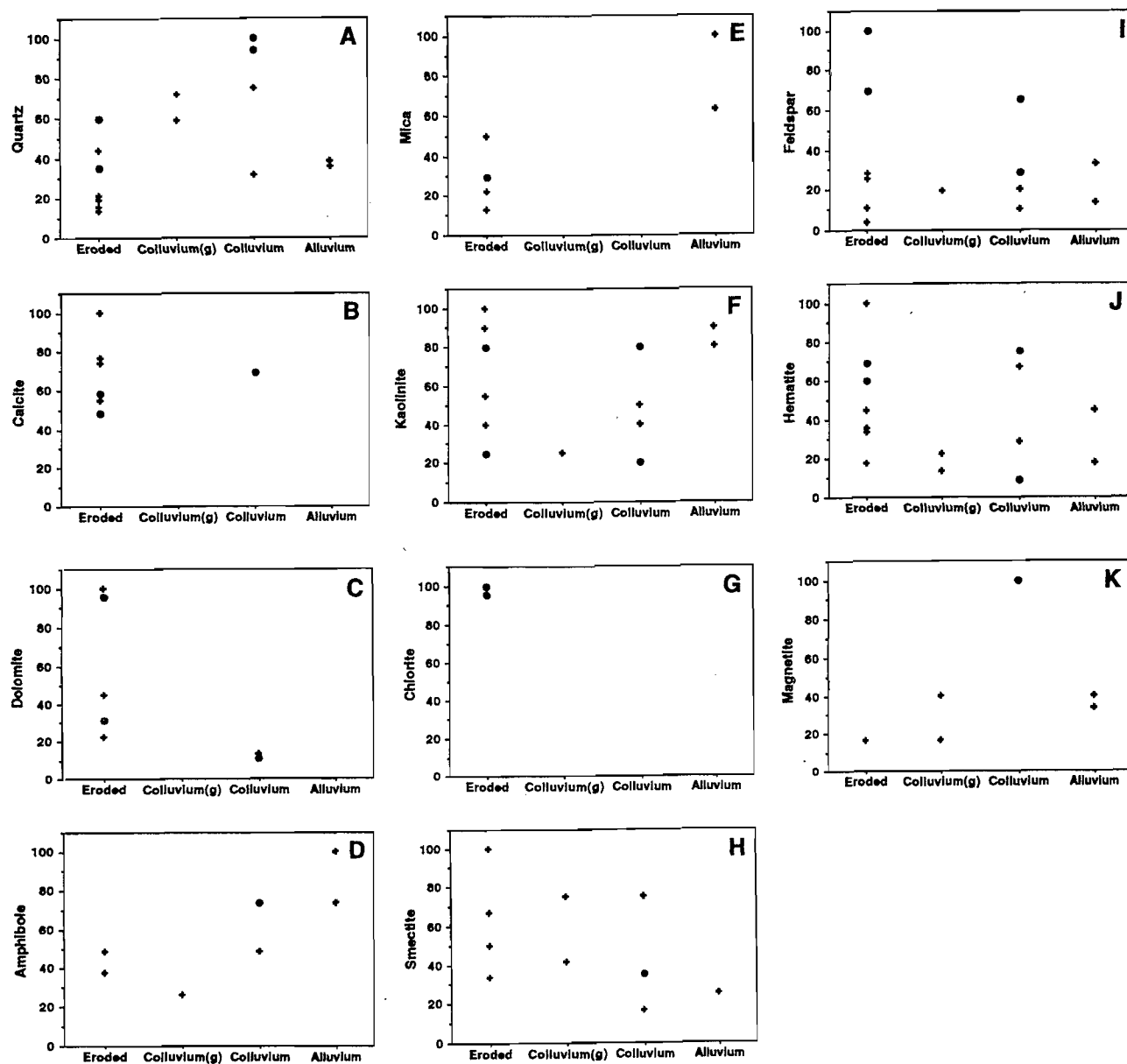
Figure 8. Relative mineral composition of soils from the eroded, colluvial and alluvial environments. Gilgai soils (g) are shown separately as are the coarse and fine soil fractions. The mineralogical data have each been rescaled to a percentage of maximum measured. Cross-comparisons between minerals should not be attempted.

6.2 Size fraction analysis

Five sub-samples from soils which represented different geomorphological environments were wet sieved into their principal fractions (>2000, 710-2000, 500-710, 250-500, 75-250, <75 µm) and dried. Each size fraction was weighed to determine its relative abundance and practicality of later batch treatment.

The soil size distributions are quite distinctive (Table 1; Figure 7) and characterise the geomorphic environments. Those from the *erosional* regime (LE14 and 17) contain significant coarse and fine fractions (20-40%) with much less (5-15%) in the 250-710 µm range. This appears to represent a range of coarse rock and mineral fragments and a separate population (Figures 7E and F) of weathered products (silt and clay).

Those from the *colluvium* (LE23 and 32) have fine fractions (<75 µm) that make up 60-70% of the sample (Figures 7C and D) and contrasts strongly with the cobble-rich lag which overlies it (Figures 4C and D). This weakly bimodal distribution seems to reflect coarse material brought in by sheet wash, together with some transported fine, weathered material to which have been added fine, partly weathered materials from the basement, brought in by soil bioturbation. The gilgai soils have a similar size distribution (Figure 7B) but lack any lag overlay.

The *alluvium* is quite distinct and has a mode in the silty 75-250 µm fraction, with a bell-shaped distribution (Figure 7A), typical of sorting in an aqueous environment. This suggests a slow current velocity (about 0.3 m/s; Leeder, 1982) during summer floods (probably flood plain or overbank environment), with very little over 500 µm.

TABLE 1
WEIGHT PERCENT OF SIZE FRACTIONS

FldNo	>2000 µm	710-2000 µm	500-710 µm	250-500 µm	75-250 µm	<75 µm	Environment
LE07	1.6	6.9	5.4	21.1	49.2	15.8	Alluvial
LE14	39.7	10.3	1.8	4.3	11.8	32.1	Erosional
LE17	39.7	17.3	4.6	8.0	13.2	17.3	Erosional
LE23	11.7	4.7	1.2	4.1	15.2	63.0	Colluvial
LE32	6.2	2.3	0.8	3.0	16.6	71.1	Colluvial

6.3 Mineralogy

The mineralogy of selected soil samples and size fractions was determined semi-quantitatively and the results presented in Table 2 and plotted in Figure 8. As expected, the fine fractions (<75 µm) are richer in kaolinite, smectite and calcite, and poorer in quartz and feldspar than the coarse fractions (710-2000 µm).

Chlorite (Figure 8G) only occurs in the coarse fraction of the soils derived from the eroded basement, presumably as fragments of chloritic schist. Mica (muscovite and/or biotite) occurs in both fractions of soil (Figure 8E) from the eroded basement and, more abundantly (probably largely as muscovite) in the dominant, fine fraction of the alluvium but is absent from the colluvium.

The carbonates, calcite and dolomite (Figures 8 B and C), occur most abundantly in the soil on the eroded basement where they are derived both from primary carbonate (veins and pods) as well as from secondary calcrete. Carbonates are less abundant in the colluvium (in two samples) and are absent from the 'gilgai' soils and the alluvium.

Feldspar (Figure 8I), as plagioclase (3.18-3.22 Å XRD reflections) is most abundant in the coarse fraction of the soils on the eroded basement, is present in the colluvium, but less so where 'gilgai' soils are developed; lesser amounts of feldspar, largely as microcline, occur in the alluvium.

Hematite (Figure 8J), in large part from weathering of magnetite (Figure 8K), is present in the soil from the eroded basement and in the colluvium but is less abundant in the 'gilgai' soils and alluvium.

In summary, the 'gilgai' soils are characteristically rich in smectite and quartz, poor in kaolinite, feldspar and hematite and free of mica and carbonates. The alluvium is rich in amphibole, mica and kaolinite, is poor in smectite, hematite, feldspar and quartz, and free of carbonates and chlorite. Compared to the soils on the eroded basement, the soils on the colluvium ('gilgai' soils excepted) are slightly poorer in kaolinite, smectite, hematite and feldspar but richer in quartz, amphibole and magnetite.

7 SOIL GEOCHEMISTRY

7.1 Bedrock target anomaly

The Cu distribution in bedrock, as supplied by CRAE (Figure 9), shows a north-striking anomalous band about 300 m wide and over 1 km long that extends for a short distance below the alluvium of Cabbage Tree Creek. Although the highest Cu abundances were located below and on the edge of the colluvium to the south (25 000 ppm), significant Cu concentrations (5000 ppm) occur near the Little Eva shaft and in the erosional regime. This well-established bedrock Cu anomaly is the target of the orientation soil geochemical survey.

7.2 Sources and assessment of field contamination

A cattle pen is located on the alluvial unit to the north-west of Cabbage Tree Creek (Figure 3). Likely contaminating materials that could be incorporated into the soil are from *cattle feeds and licks*, which consist of salt (Na, K, Rb, Cs), gypsum (Ca, S), rock phosphate (P, U, REE) and necessary trace elements (Zn, Cu, Se, Mo). Sodium would be readily flushed from the soil during summer rains. Rock phosphate would be less readily removed and would be dispersed in the soil by the trampling of cattle.

Streams, feeding Cabbage Tree Creek from the south, drain the environs of the Dugald River Lode, some 12 km away. Thus, they may contain a stream sediment signature from a significant Zn-Pb deposit. Stream sediment geochemical information, supplied by CRAE, was used to investigate dispersion of Pb and Zn along these streams by plotting their elemental abundances against the northings of the sample locations (Figure 10). Although, near the Dugald lode, the stream sediments contain >100 and >1000 ppm Pb and Zn respectively, their abundances are reduced to background within a few km and are near 10 ppm for both elements in the vicinity of Little Eva. Thus, the geochemical contribution from the Dugald River Zn-Pb lode to modern sediments near Little Eva is not significant.

24
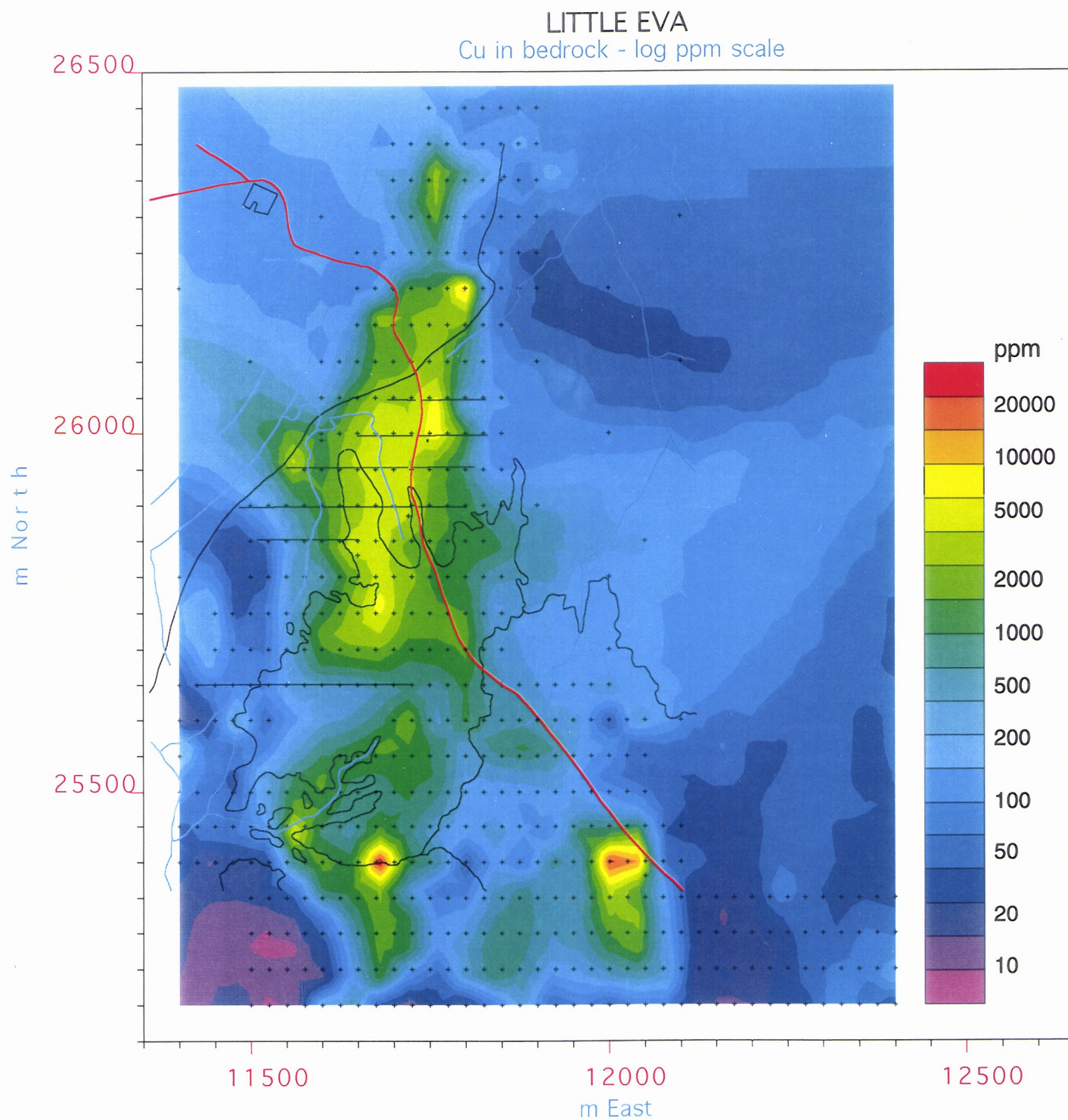
Figure 9. Copper distribution in bedrock (data supplied by CRAE). CSIRO regolith mapping has been superimposed (see Figure 3 for explanation).
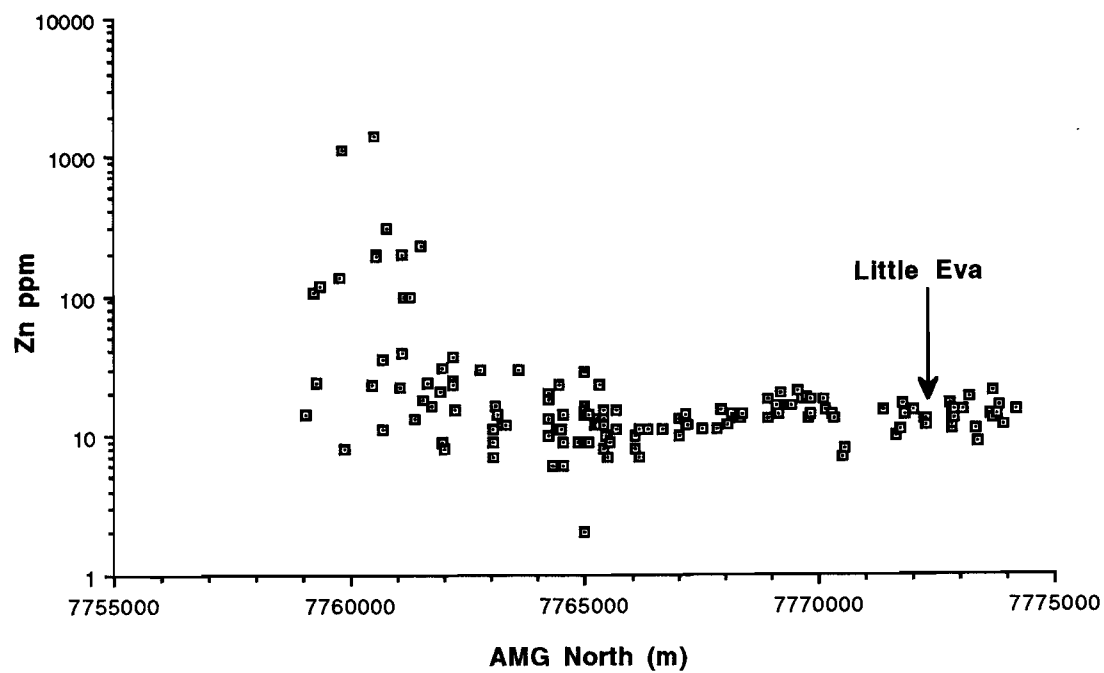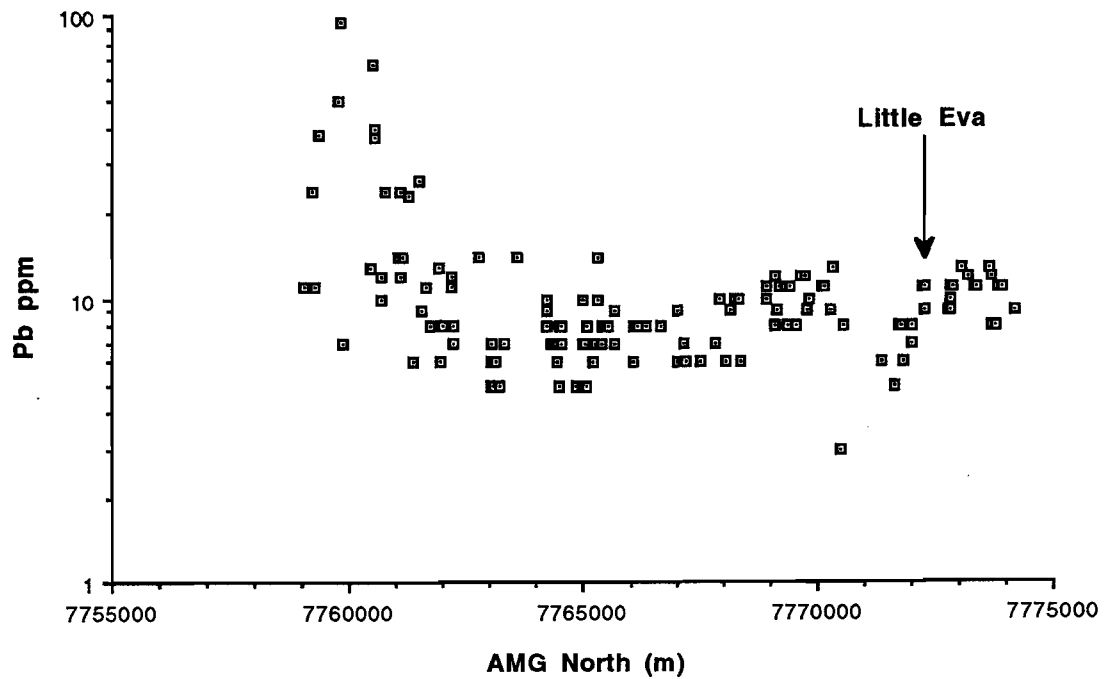
Figure 10. Scatter plots of Pb and Zn stream sediment data plotted against northing from an area bounded by 411000E-413000E and 7759000-7774400N; Zone 54 AMG. This data covers the drainages flowing north from near the Dugald River Lode towards the Little Eva Cu Prospect. Data supplied by CRAE.

7.3 Pilot study

Five sub-samples from soils which represented different geomorphological environments (namely; erosional and depositional) were selected for pilot treatment from material used for the size fraction analysis. Of these, only four fractions (>2000, 710-2000, 250-500 and <75 μm; LE–14, 17, 23 and 32) were selected for analysis. The results are presented in Table 3. Geochemically, the >2 mm fraction would be difficult to use, as it contains pebbles of probable exogenous origin reaching >25 mm in diameter and would require a very large sample size to be representative. This fraction was regarded as of little value as a geochemical medium. The multi-element properties of the remainder were assessed for important target, pathfinder and lithological indicator elements to select the best fraction or fractions for further assessment.

Twenty four elements, including As, Au, Cu and Zn, showed the widest compositional ranges in the fine (<75 μm) fraction (Table 3). This was closely followed by the coarse (710-2000 μm) fraction (19 elements, including Ag, Mn, Ba, Mo, Pb, S and Sb); the 250-500 μm fraction showed the greatest range in only four elements (Si, Fe, Bi and Cr). Among the target and pathfinder elements, the maximum values were generally shown by the <75 μm fraction and partly by the 710-2000 μm fraction (Table 3). The best fraction was again the <75 μm fraction and this is illustrated in Figure 11. Thus, these two size-contrasted fractions were selected for analysis and comparison. Selection of the coarse and fine fractions seemed particularly relevant in view of the contrasted and possible exogenous origin of the coarse lag on the colluvium and the possibility of hydromorphic dispersion and bioturbation influencing the fine fraction.

7.4 Soil survey

The soil data are tabulated in Appendices 1 and 2 and have been contoured in Appendix 3. Appendix 7 contains a removable, transparent, regolith map for use with Appendix 3. Particularly relevant plots (Cu, Au, Ca, Fe, Co, V, P, Yb) are duplicated in colour in Figure 12.

The small number of samples in the data set (34) and their derivation from at least three contrasted environments prevented satisfactory statistical data analysis and determination of anomaly thresholds. However, approximate thresholds can be estimated retrospectively from the contoured data.

Copper
Very similar Cu results were obtained in both soil fractions (Figures 12A and B). Because of the highly skewed nature of the population, the Cu data have been plotted on a logarithmic scale. Maximum abundances are greater in the fine fraction by half an order of magnitude. As would be expected, the exposed area south of the Little Eva shaft is targeted very clearly. However, there is a distinct ridge in the soil Cu distribution, about an order of magnitude less than in the exposed area, which reflects the overall trend of the bedrock Cu anomaly under the thin colluvial mantle (Figure 9). The north-east part of the sampled area, covered by alluvium, lacks any Cu anomaly, with Cu abundances close to the detection limit (10 ppm).

Gold
Gold in both fractions accurately targets the same locality in the erosional regime as the Cu with a bullseye anomaly. This is centred at 11720E-25900N with a weak trend to the south, in the fine fraction, under the colluvium. This is best shown on a log plot which places more emphasis on lower values. Logarithmic treatment of the Au in the coarse fraction gives little improvement (Figure 12D). Gold is an important pathfinder because small quantities of Au occur with the primary mineralisation.

TABLE 3
PILOT STUDY

FieldNo Element UNITS Detn	Type	Fraction μm -	North m -	East m -	XRF(f) SiO2 % 0.01	XRF(f) Al2O3 % 0.01	XRF(f) Fe2O3 % 0.01	XRF(f) MgO % 0.01	XRF(f) CaO % 0.001	XRF(f) Na2O % 0.01	XRF(f) K2O % 0.001	XRF(f) TiO2 % 0.003	XRF(f) MnO % 0.002	XRF(f) P2O5 % 0.002	XRF(f) Iod % -	XRF(f) loi % -	GS201 Ag ppm 0.1	INAA As ppm 1.0	INAA Au ppb 5	XRF(f) Ba ppm 30	GS201 Bi ppm 0.10	INAA Br ppm 2.0	GS201 Cd ppm 0.1	INAA Ce ppm 2.0	XRF(f) Cl ppm 20	INAA Co ppm 1	INAA Cr ppm 5	INAA Cs ppm 1.0	XRF(f) Cu ppm 10
LE14A	Eros	>2000	26000	11800	40.42	8.84	7.61	0.99	19.78	3.70	0.71	0.57	0.029	0.035	0.57	16.63	0.3	1.1	11	47	0.05	3.9	0.1	19.8	100	14	37	0.5	149
LE14B	Eros	710-2000	26000	11800	45.10	9.53	11.90	2.06	12.90	2.97	1.60	0.80	0.046	0.031	1.04	11.99	0.2	1.4	18	140	0.05	3.8	0.1	27.7	190	26	50	0.5	328
LE14D	Eros	250-500	26000	11800	53.81	8.33	11.67	2.09	9.80	1.91	1.79	0.88	0.045	0.028	0.77	9.15	0.3	1.3	9	223	0.05	2.9	0.1	42.4	170	27	56	1.2	340
LE14F	Eros	<75	26000	11800	30.19	8.41	7.30	2.74	22.10	0.81	0.78	0.48	0.036	0.116	3.46	23.83	0.3	1.9	48	125	0.05	20.2	0.2	38.6	190	28	45	0.5	464
LE17A	Eros	>2000	25900	11500	40.81	8.31	5.30	2.81	19.67	1.43	3.05	0.27	0.054	0.068	0.47	17.72	0.3	0.5	2	236	0.05	2.7	0.1	43.9	170	11	36	0.5	1
LE17B	Eros	710-2000	25900	11500	46.33	9.49	7.67	2.48	14.80	1.34	3.50	0.44	0.054	0.045	0.48	13.28	0.2	0.5	2	302	0.05	2.1	0.1	46.5	170	14	44	1.1	21
LE17D	Eros	250-500	25900	11500	47.27	8.77	19.87	2.46	8.70	0.85	3.11	0.62	0.051	0.036	0.50	8.25	0.2	0.5	2	314	0.20	-2.0	0.2	77.9	150	22	83	1.4	38
LE17F	Eros	<75	25900	11500	30.11	8.81	6.29	4.25	22.03	0.37	1.21	0.47	0.039	0.093	3.21	23.72	0.3	1.3	10	140	0.05	10.4	0.1	92.0	510	23	45	2.4	35
LE23A	Col	>2000	25830	11650	70.54	8.07	12.31	1.24	1.41	1.81	1.54	0.77	0.043	0.041	0.54	1.69	0.4	3.2	2	147	0.10	3.2	0.1	54.9	900	24	45	1.3	440
LE23B	Col	710-2000	25830	11650	65.68	8.69	14.86	1.93	1.09	1.59	2.02	0.97	0.106	0.034	0.83	2.35	0.5	3.1	37	237	0.10	-2.0	0.2	162.0	380	48	47	1.3	815
LE23D	Col	250-500	25830	11650	81.22	5.29	7.20	0.71	0.60	0.65	2.15	0.76	0.040	0.012	0.28	0.94	0.3	1.5	2	288	0.05	-2.0	0.1	76.2	110	17	34	1.1	324
LE23F	Col	<75	25830	11650	51.74	17.51	12.84	1.45	0.88	0.83	1.38	1.38	0.066	0.050	4.16	8.07	0.5	4.0	53	289	0.10	7.9	0.1	65.9	70	30	66	3.0	1401
LE32A	Col	>2000	25600	11700	71.53	4.25	7.30	0.61	6.88	1.14	0.93	0.31	0.186	0.031	0.29	6.40	0.3	2.7	16	357	0.05	4.0	0.2	45.0	520	20	26	0.5	91
LE32B	Col	710-2000	25600	11700	49.48	3.23	3.63	1.11	21.13	0.34	0.97	0.19	0.453	0.012	0.74	18.56	0.2	2.6	2	860	0.05	4.3	0.2	86.0	90	48	24	0.5	126
LE32D	Col	250-500	25600	11700	91.52	2.74	2.16	0.12	1.14	0.26	1.47	0.19	0.067	0.007	0.04	0.88	0.2	1.4	2	333	0.05	-2.0	0.1	25.2	110	6	25	0.5	24
LE32F	Col	<75	25600	11700	62.77	12.44	6.76	1.78	1.54	0.69	1.57	1.04	0.078	0.027	4.99	6.64	0.3	2.8	24	488	0.10	8.4	0.1	69.3	160	18	62	2.8	252
Range	-	>2000	-	-	31.11	4.59	7.01	2.20	18.37	2.56	2.34	0.50	0.157	0.037	0.28	16.04	0.1	2.7	14	310	0.05	1.3	0.2	35.1	800	13	19	0.8	439
Range	-	710-2000	-	-	20.58	6.30	11.23	1.37	20.04	2.63	2.53	0.78	0.407	0.033	0.56	16.21	0.3	2.6	35	720	0.05	6.3	0.1	134.3	290	34	26	0.8	794
Range	-	250-500	-	-	44.25	6.03	17.71	2.34	9.20	1.65	1.64	0.70	0.027	0.029	0.74	8.26	0.1	1.0	7	110	0.15	4.9	0.1	52.7	60	20	58	0.9	316
Range	-	<75	-	-	32.66	9.10	6.55	2.80	21.22	0.46	0.79	0.91	0.042	0.089	1.78	17.19	0.2	2.8	43	363	0.05	12.3	0.1	53.4	440	12	22	2.5	1366

Maxima outlined for fractions excepting >2000 μm

28

TABLE 3 (Contd)
PILOT STUDY

| FieldNo	INAA	XRF(f)	INAA	INAA	INAA	INAA	GS201	XRF(f)	XRF(f)	XRF(f)	XRF(f)	XRF(f)	INAA	INAA	INAA	INAA	XRF(f)	INAA	INAA	INAA	XRF(f)	INAA	XRF(f)	INAA	XRF(f)	XRF(f)
Element	Eu	Ga	Hf	Ir	La	Lu	Mo	Nb	Ni	Pb	Rb	S	Sb	Sc	Se	Sm	Sr	Ta	Th	U	V	W	Y	Yb	Zn	Zr
UNITS	ppm	ppm	ppm	ppb	ppm	ppm	ppm	ppm	ppm	ppm	ppm	ppm	ppm	ppm	ppm	ppm	ppm	ppm	ppm	ppm	ppm	ppm	ppm	ppm	ppm	ppm
Detn	0.50	3	0.50	20	0.5	0.20	0.10	4	10	5	20	10	0.20	0.10	5	0.20	5	1.0	0.5	2.0	5	2	5	0.50	5	5
LE14A	0.52	10	2.21	<20	10.2	0.22	0.40	1	9	5	19	70	0.10	13.00	<5	1.94	39	1.3	2.4	1.0	169	6	11	1.41	6	77
LE14B	0.57	11	2.43	<20	11.3	0.21	0.80	0	39	7	50	90	0.10	13.30	<5	2.21	37	1.3	5.0	2.5	194	1	13	1.67	14	97
LE14D	0.54	11	2.43	<20	18.6	0.22	0.70	1	38	7	65	70	0.10	14.20	<5	2.61	40	1.1	6.4	1.0	183	1	14	1.63	11	87
LE14F	0.74	10	5.37	<20	20.3	0.29	0.30	3	39	4	35	220	0.30	14.90	<5	3.65	45	1.1	7.0	1.0	122	1	17	2.10	19	228
LE17A	0.83	10	2.49	<20	26.6	0.27	0.30	0	4	2	90	60	0.10	8.66	<5	4.17	95	0.5	7.6	1.0	85	1	17	2.05	7	79
LE17B	0.89	10	2.41	<20	25.7	0.26	0.60	1	19	5	114	70	0.10	10.10	<5	3.90	70	0.5	7.4	1.0	88	1	19	1.78	5	89
LE17D	1.05	15	2.48	<20	31.0	0.25	0.60	1	36	4	110	70	0.10	12.50	<5	4.40	58	1.8	8.3	1.0	221	1	16	2.02	5	92
LE17F	1.53	13	5.65	<20	49.2	0.31	0.20	4	12	3	69	170	0.10	15.10	<5	7.65	101	0.5	9.6	1.0	116	1	26	2.39	13	211
LE23A	0.91	11	2.32	<20	25.1	0.25	1.50	2	37	10	50	80	0.59	14.90	<5	4.29	64	1.1	5.2	1.0	221	1	18	2.04	11	89
LE23B	1.37	13	2.61	<20	22.5	0.27	2.50	1	54	15	74	60	0.45	15.80	<5	3.63	62	0.5	5.2	3.5	287	1	17	2.13	10	89
LE23D	0.57	8	1.90	<20	17.0	0.10	1.50	1	20	10	73	60	0.10	7.28	<5	2.34	35	0.5	4.2	1.0	144	1	10	1.19	4	63
LE23F	1.69	22	9.89	<20	42.0	0.60	0.60	7	50	10	74	110	0.43	27.10	<5	6.85	56	1.3	11.6	2.1	269	1	34	4.10	21	385
LE32A	1.61	5	2.28	<20	47.7	0.27	2.70	5	27	8	33	130	0.53	4.49	<5	6.88	82	1.3	4.9	1.0	140	1	27	2.11	14	83
LE32B	3.22	3	1.98	<20	108.0	0.35	1.20	0	26	2	38	200	0.25	3.93	<5	14.30	205	0.5	3.1	1.0	110	1	54	2.92	10	70
LE32D	0.20	5	1.39	<20	13.1	0.10	1.30	3	10	8	48	60	0.31	2.07	<5	2.01	24	0.5	3.5	1.0	37	1	7	0.67	4	46
LE32F	1.27	16	10.70	<20	28.6	0.52	0.30	8	25	13	87	100	0.36	15.40	<5	5.77	90	2.1	13.2	1.0	131	1	30	3.65	26	413
Range	1.09	6	0.28	0	37.5	0.05	2.40	5	33	8	71	70	0.49	10.41	0	4.94	56	0.8	5.1	0.0	136	5	16	0.70	8	12
Range	2.65	10	0.63	0	96.7	0.14	1.90	1	35	13	76	140	0.35	11.87	0	12.09	168	0.8	4.3	2.5	199	0	41	1.25	9	27
Range	0.85	10	1.09	0	17.9	0.15	0.90	2	28	6	62	10	0.21	12.13	0	2.39	34	1.3	4.9	0.0	184	0	9	1.35	7	46
Range	0.95	12	5.33	0	28.9	0.31	0.40	5	38	10	52	120	0.33	12.20	0	4.00	56	1.6	6.2	1.1	153	0	17	2.00	13	202
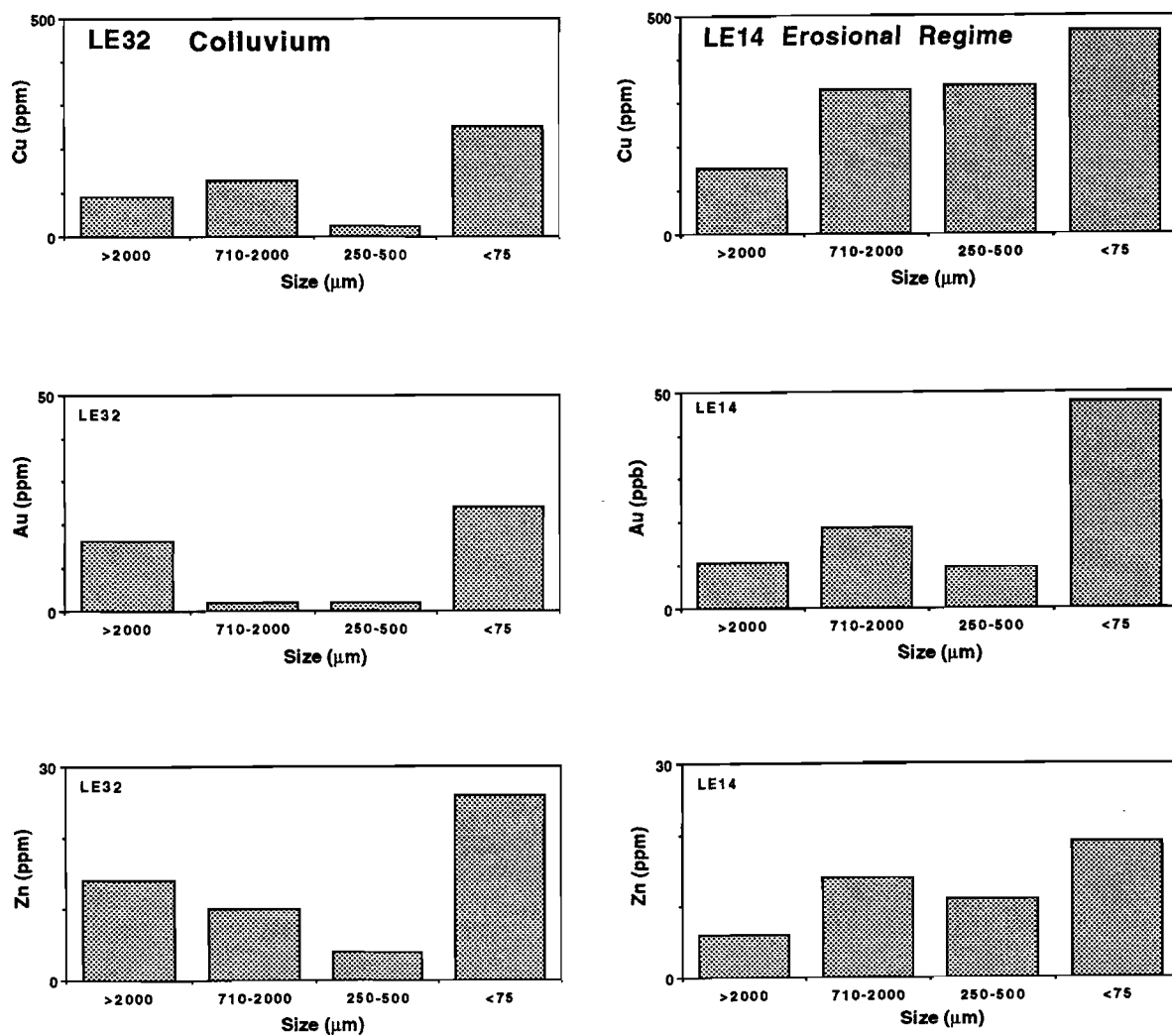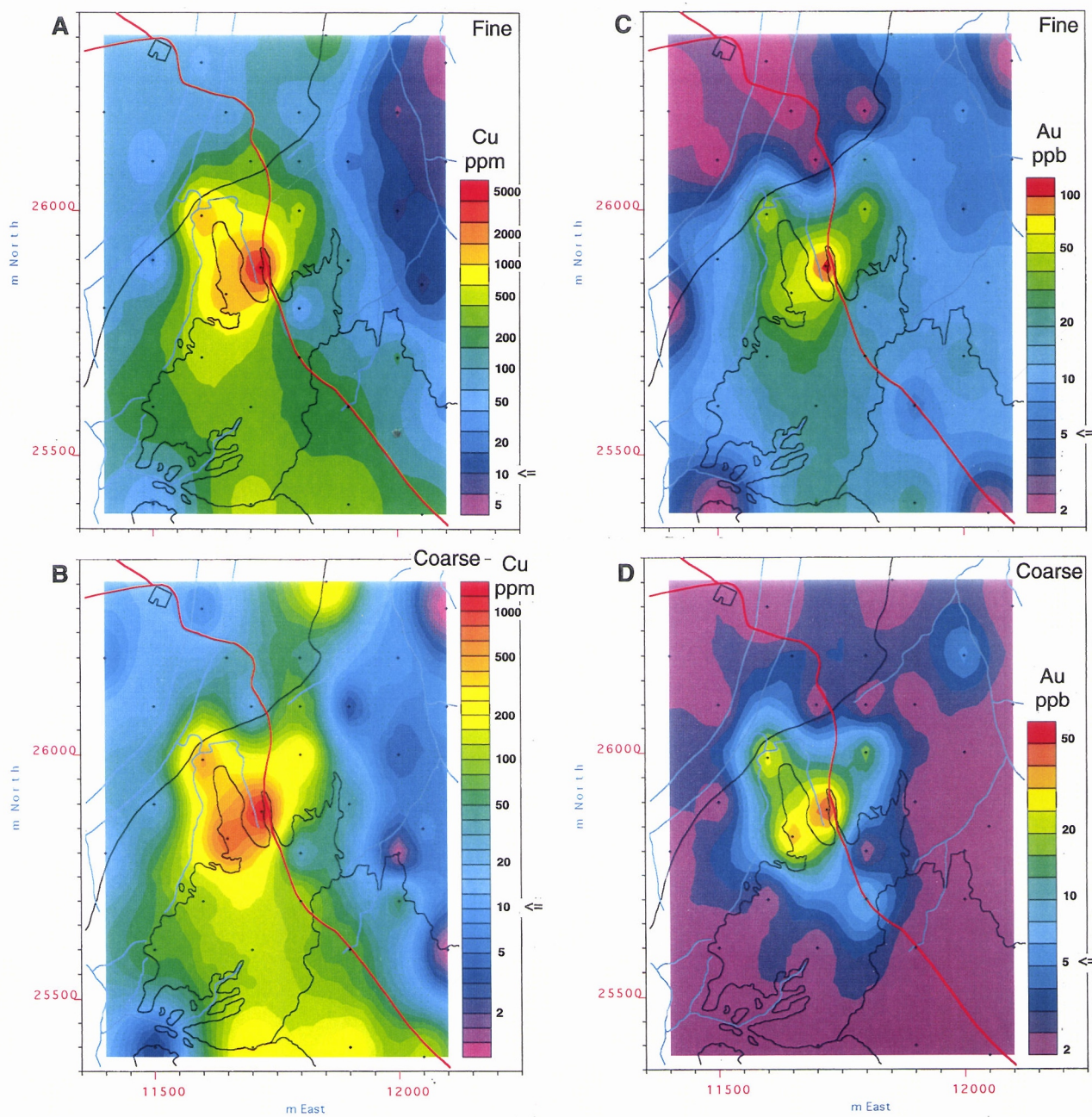
Figure 11. Histograms comparing the abundances of Cu, Au and Zn in four size fractions in the depositional and the erosional regimes. The strongest geochemical signals come from the fine fractions.
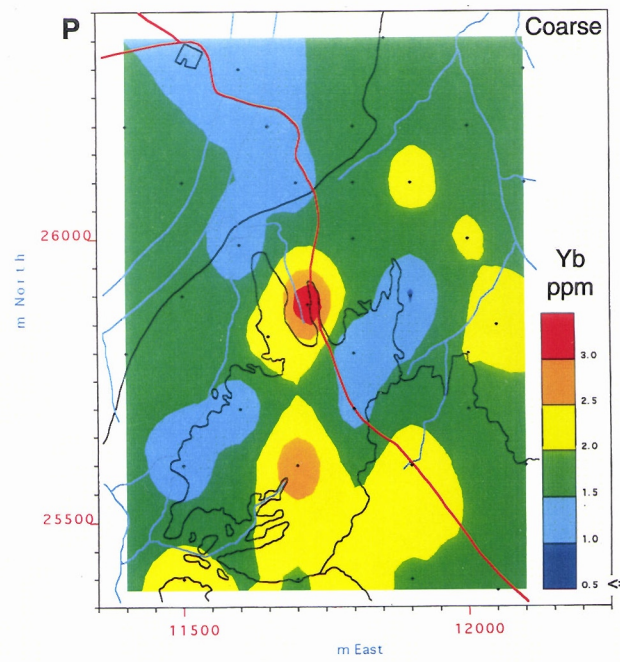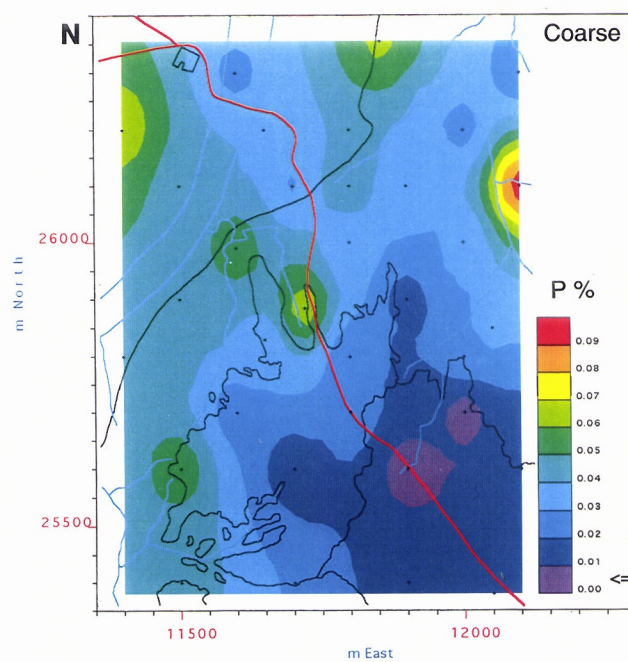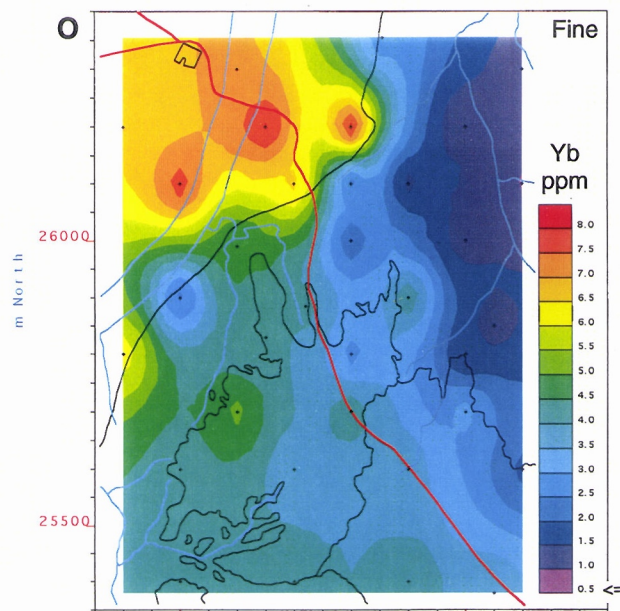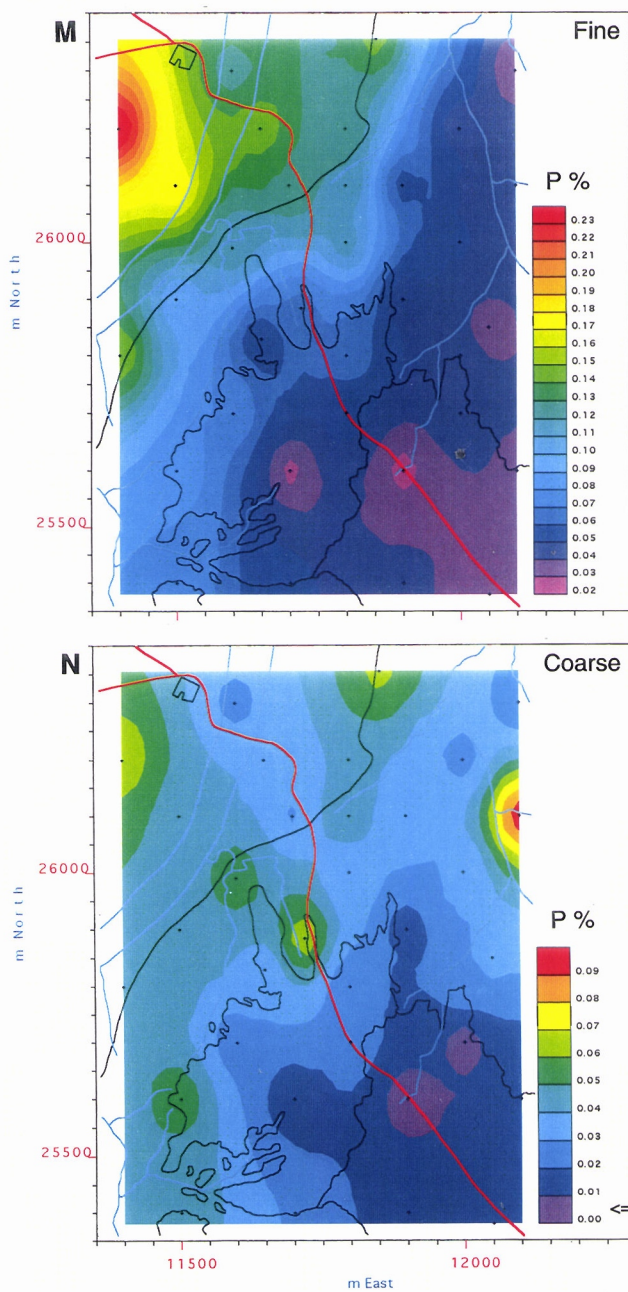
Figures 12A-D. Colour contour plots of soil geochemical data for Cu and Au. Logarithmic contouring used. Detection limit shown <= .
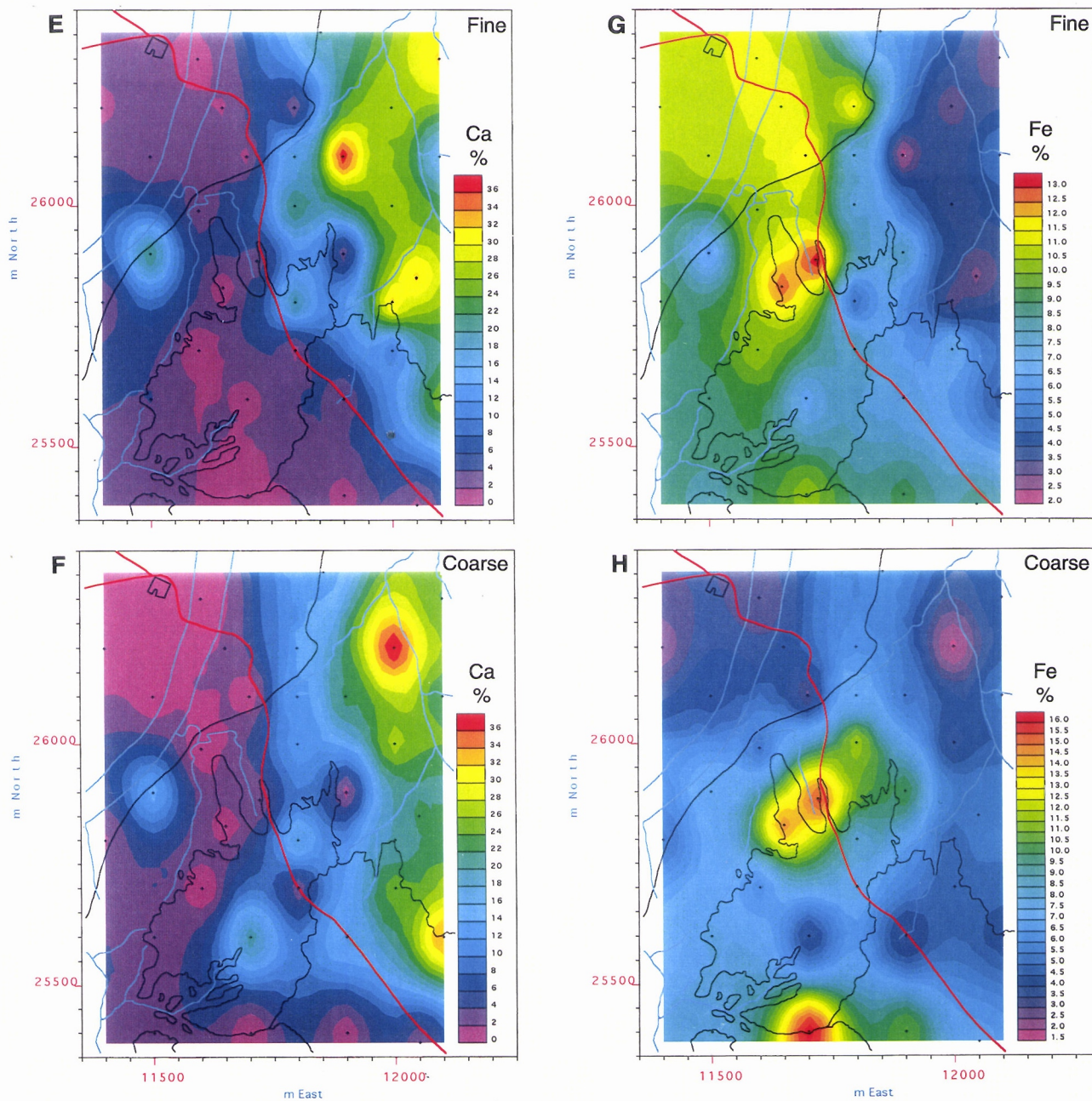
Figures 12E-H. Colour contour plots of soil geochemical data for Ca and Fe expressed as oxide%.
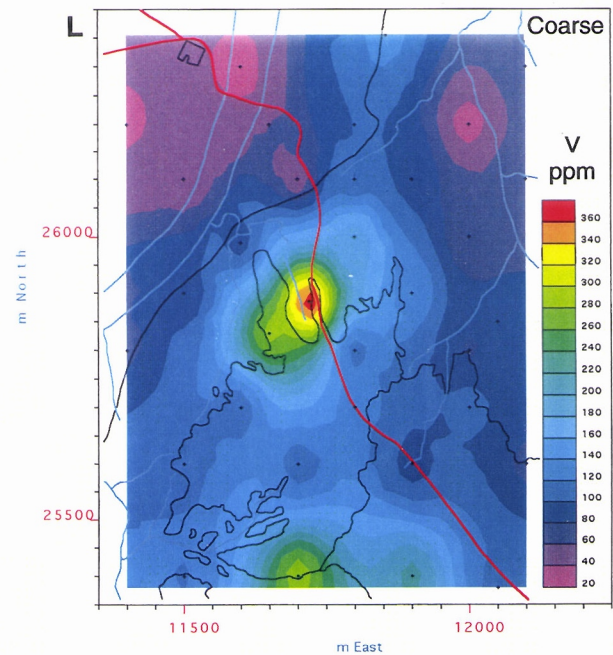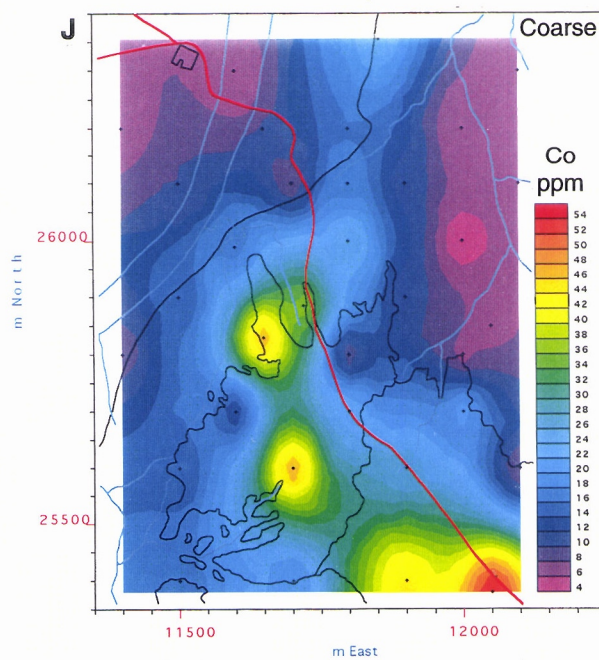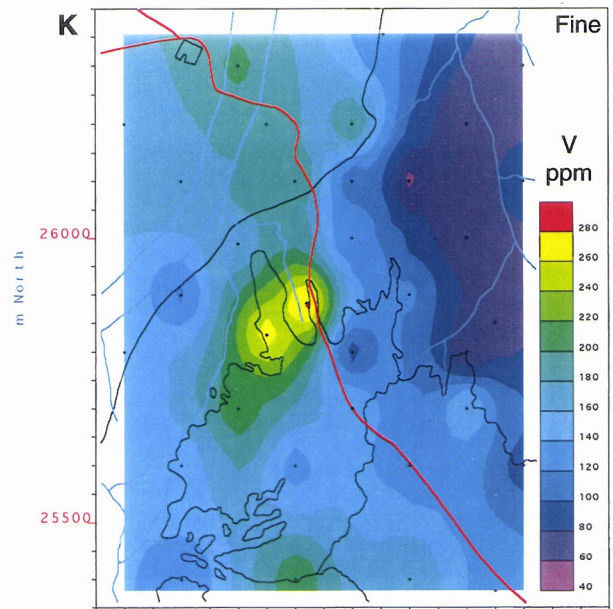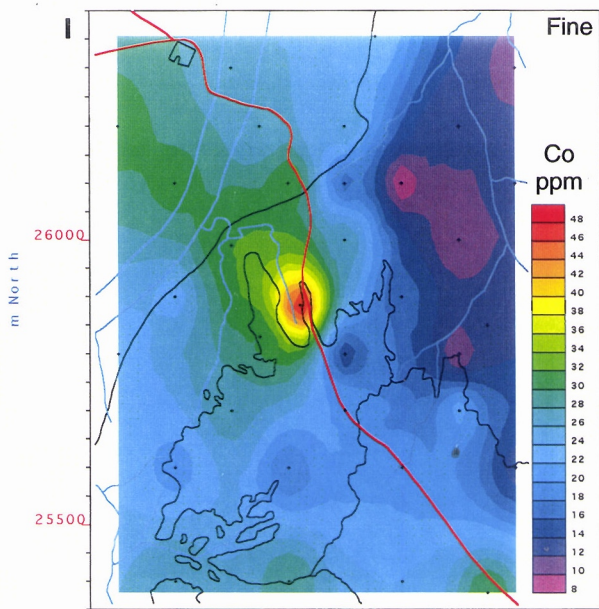
Figures 12I-L. Colour contour plots of soil geochemical data for Co and V.

Figures 12M-P. Colour contour plots of soil geochemical data for P, expressed as oxide% and Yb in ppm. Detection limits shown as <= .

Lead and Zn

The exposed basement in the east of the sampled area is particularly poor in Pb (<6) and Zn (<15) in both soil fractions (Appendix 3); such Pb and Zn abundances are typical of carbonate and psammitic rocks. The Pb concentrations in the colluvium are generally >10 ppm. The Pb concentrations in the alluvium, in both the coarse and fine fractions, are typical of a granitic provenance (15-20 ppm). There is a probably false single-point Zn concentration of 125 ppm in the fine fraction in the alluvium about 200 m south-west of the cattle pen; this coincides with a P concentration in the same fraction which is probably related to stock feed supplements trampled into the soil by the cattle. The remainder of the alluvium has a Zn concentration of 60 ppm. No Pb or Zn soil anomalies are associated with the Little Eva Cu-Au mineralisation.

Major elements (Si, Al, Fe)

The soils are largely composed of Si, Al and Fe (Appendix 3) and this is expressed by the Si-Al-Fe ternary diagrams (Figure 13). All are highly siliceous.

Among the coarse fractions of the soils, the most siliceous is alluvium (Figure 14). Slightly greater Fe contents are displayed by the others, the most aluminous being those overlying the basement (Figure 14) due to abundant primary Al-silicates (principally feldspars).

The fine fractions (Figures 13 and 14) are all closely comparable; the most Al- and Fe-rich is the alluvium. Soils on the basement and on the overlying colluvium also have variable Ca and Mg contents (Figures 12E and F; Appendix 3), although Ca dominates (Figure 14), reflecting their carbonate contents; Mg is probably contained mainly in ferromagnesian minerals and smectites.

However, superimposed on this Fe variance, is a marked Fe anomaly (>12% Fe_2O_3) in both fractions centred at 11720E-25900N (Figures 12G and H). This coincides with similar soil anomalies in Cu and Au and probably relates to increased magnetite concentrations in the soil around the mineralised system. This is particularly evident in the coarse soil fraction, where a second Fe anomaly at 11700E 25400N marks bedrock Cu concentrations of >10 000 ppm. However, neither Cu nor Au is concentrated with the magnetite (Section 7.5).

Alkaline Earths (Ca, Mg, Ba)

Spatially, high Ca concentrations (12->30% CaO) in both fractions are restricted to the north-east part of the exposed basement and reflect the development of calcrete in this area (Figures 12E and F). This may reflect a high primary Ca content, given the high proportion of coarsely crystalline primary calcite in the soil from this region. In contrast, the distribution of Mg (Appendix 3) is more closely related to the outcrop of the basement as a whole, probably reflecting the amphibole content of the granofelses. The distribution of Sr is more closely related to Ca than to Mg, as would be expected.

Dilution of the soils by carbonates has had a considerable influence on the distributions of Si, Al and Fe. They have a spatially converse relationship and this is particularly evident in the fine fraction. This converse relationship among major elements, due to closure, has had an unduly strong influence on inter-element correlations throughout the data set (Appendix 6). An example is Ga, which is strongly correlated with Al. Thus Ga also has an inverse correlation with Ca and hence with Sr. Barium (Appendix 3) shows a similar distribution to Mn in both soil fractions and is unrelated to the other alkaline earths.

Transition elements (Co, V, Mn, Cr, Ni, Ti, Zr, Hf)

The transition elements Co (Figures 12I and J) and V (Figures 12K and L) have distributions related to those of Cu, Au and Fe (Figures 12A-D; G and H). All fractions show an anomaly near to 11700E 25400N. Vanadium in both fractions and Co in the coarse fraction all show a north-striking ridge structure that may be related to mineralisation. The magnetic fraction of the soil
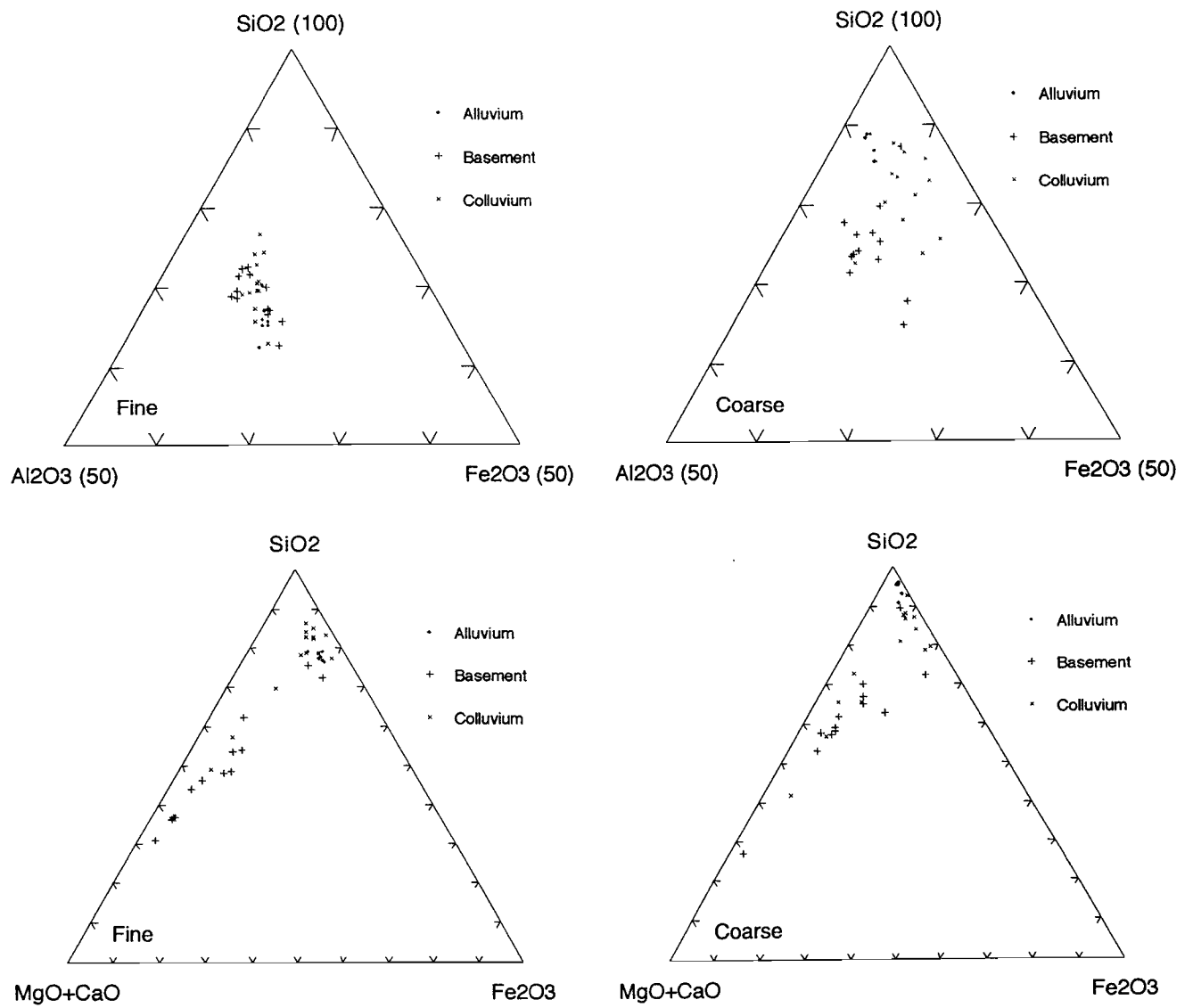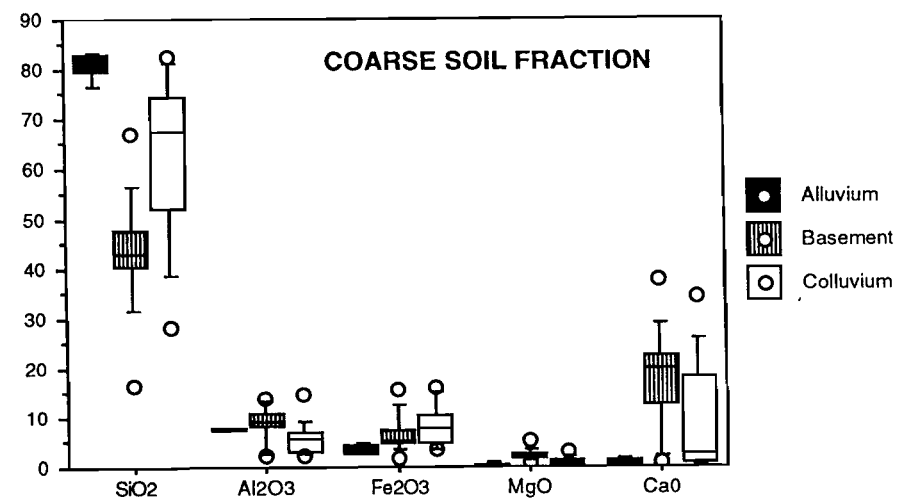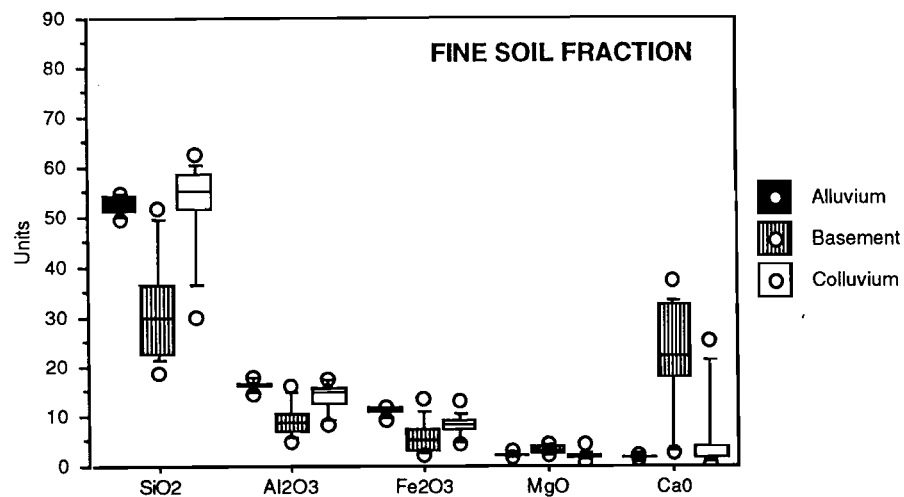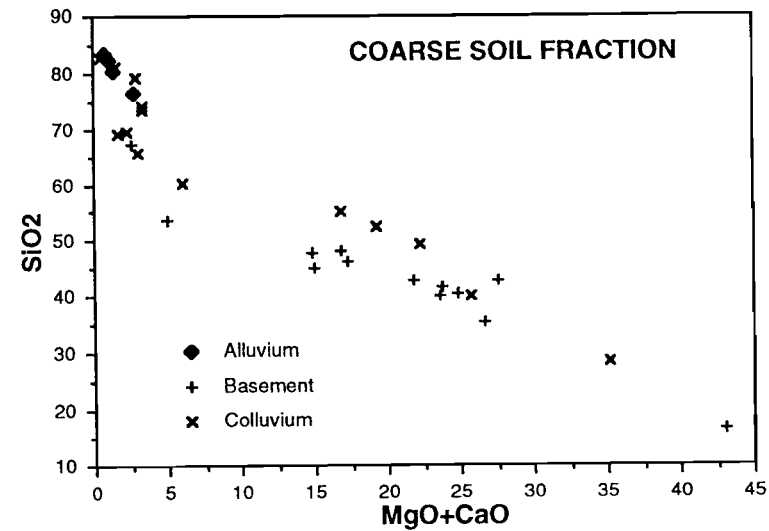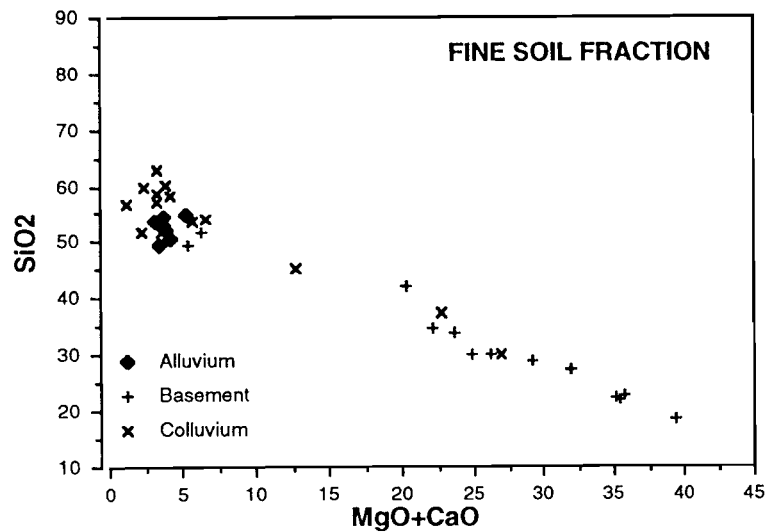
35

Figure 13. Ternary diagrams of major element compositions of soil.

Figure 14. Major element scattergrams and box-plots.

contains elevated V and Co, the plot suggesting that most of the V and at least some of the Co are located in magnetite (Section 7.5).

The greater concentrations of Mn (>0.2% MnO) in the coarse soil fraction (Appendix 3) mainly occur in the colluvial area in the south-east, at least in part associated with areas of cracking clays. The fine soil fraction on the exposed basement is characteristically Mn poor (<0.1 MnO) compared to the colluvium and alluvium (>0.1% MnO). Maximum concentration in the fine soil fraction (0.2% MnO) is significantly less than that of the coarse soil fraction (0.6% MnO). The reasons for the greater concentrations in colluvium are, as yet, unexplained.

Chromium and Ni (Appendix 3) show very similar patterns. In the coarse fraction, they both show a spot high close to the road on the boundary between the two colluvial units. In the fine fraction, this spot high is displaced to the east by 200 m. The reasons for these are not known. The magnetic fraction (Section 7.5) contains elevated Cr and Ni, suggesting that at least a significant proportion, although not all, of these elements are held in the spinel structure or adsorbed on secondary Fe oxides clinging to the spinel.

The Ti distribution (Appendix 3) in the coarse soil fraction is very similar to that of Fe; in the fine soil fraction, the greatest Ti concentrations occur in the alluvium. Titanium probably occurs partly as ulvospinel in the soil magnetite, as ilmenite (also in the magnetic fraction) and in mafic minerals (biotite, chlorite, hornblende).

The Zr and Hf distributions (Appendix 3) are very similar. As for Ti, the greatest concentrations in the fine soil fraction occurs in the alluvium and the least on the eastern part of the exposed basement. The coarse soil fractions for both these elements are lesser by almost an order of magnitude. These elements probably occur as detrital ilmenite (Ti) and zircon (Zr, Hf).

Halogens and sulphur
The halogens Cl and Br and, to some extent, S are restricted to exposed parts of the basement (Appendix 3), in the east, which could reflect the presence of small quantities of scapolite[2]. Although Br is not normally included in the scapolite formula, it could replace Cl; Br⁻ is smaller than CO_3 and could easily be accommodated in the scapolite structure (R.A. Eggleton, 1995; pers comm). Absence of these elements in the exposed area to the north of Little Eva could reflect stratigraphic variations in the scapolite content of the granofelses.

Alkalis (Na, K, Rb, Cs)
The heavier alkalis (K, Rb, Cs) show almost identical patterns in both fractions. The basement in general and, particularly, the eroded basement in the eastern part of the sampled area are poor in these alkalis, indicating a comparative lack of mica and K feldspar. No phyllic halo associated with the mineralisation was detected in the soil. The areas mantled by colluvium are comparatively poor in these elements. In contrast, higher concentrations in alluvium reflect detrital mica and K feldspar and the concentrations are typical for a granitic provenance. The alkali enrichment, particularly in the coarse fraction, in a sample located at 11500E 25400N (Sample LE31) is largely due to a localised accumulation of mica. Sodium shows an anomaly in the coarse soil fraction, which is weakly reflected in the fine fraction in the basement, centred at 11600E 26000N.

Metalloids (Se, As, Sb, P)
The Se content for all samples was below detection (<5 ppm). Although As and Sb contents were above detection (1.0 and 0.2 ppm respectively), the maximum abundances in the soils are

---

[2]Scapolite: $(Na,Ca,K)_4(Al_3(Al,Si)_3Si_6O_{24}(Cl,CO_3,SO_4,OH)$

generally low (8 and 0.9 ppm respectively). Their distributions do not seem to have any relationship to mineralisation and probably reflect geochemical 'noise'.

The fine soil fraction shows a considerable concentration of P (Figure 12M) in the north-west of the sampled area. In general, the alluvium is P rich (0.13% P_2O_5) but a concentration of twice this amount occurs south-west of the cattle pen at 11500E 26300N. This coincides with a Zn anomaly (see above) and probably represents contamination of the soil by cattle feed supplement (Section 7.2). The remainder of the area (basement and colluvium) is P poor. This is not really apparent in the coarse fraction.

Rare earths (Y, La, Ce, Eu, Sm, Lu, Yb) and Th
This group of lanthanides and actinides show quite similar distributions in the fine fraction. In each, the soils over the exposed basement are poor in REEs. Among the heavy REEs (Yb, Lu and Th), and Y, the alluvium carries the highest concentrations (Figures 12O and P). This is less clear in the light and intermediate REEs (La, Ce, Sm, Eu). The abundances of all REEs in the alluvium and, to some extent, the colluvium are typical of a granitic provenance. These distributions are similar to those of Mn and Ba. REE abundances in the coarse soil fraction are generally less and very patchy. There does not appear to be any relationship of the REEs to the bedrock Cu anomaly.

Incompatible elements (U, Ta, Nb, W)
The fine fraction shows the greatest concentrations of U, Ta and Nb and these depict the alluvium. In the coarse fraction, the maximum concentrations of these elements are about x2 detection limit and these data only reflect analytical 'noise'. It seems that the basement is particularly poor in these elements; the colluvium perhaps having a slightly greater abundance but these data are close to detection.

All the W data in the fine fraction lay below detection. In the coarse fraction, a single, possibly significant, anomaly of 5 ppm (DL 2 ppm) at 11700E 25400N coincides with the axis of the mineralisation and similar localised but weak concentrations in Fe, V, Ti, As and Sb in the coarse fraction. An improved detection limit (<0.2 ppm) would be necessary to assess W properly).

7.5 Magnetic concentrate

The composition of magnetic concentrates (see Section 5.2) from two samples from the axis of the bedrock Cu anomaly was investigated (Table 4). A log-log summary plot of the mean abundances of all elements of the two soil samples against the range of abundances in the magnetic concentrate (Figure 15) demonstrates which elements are carried in the magnetic material. These are all of the V, a large proportion of the Cr and much Ti, Ni, Co, Ga and Nb, showing increases of almost an order of magnitude. Most of these elements are accommodated in the spinel (magnetite) lattice (V, Ni, Ti, Co). Gallium probably occurs (with Al) in adhering goethite which may form an intimate intergrowth with the weathered magnetite (Anand and Gilkes, 1984). Predictable decreases are shown by Cu, Ba and the alkalis. Manganese, Pb and Zn are unaffected.

A magnetic concentrate from the soil does not appear to be a useful geochemical medium to detect Little Eva-style Cu-Au mineralisation. However, complete soil analysis for Fe, V and possibly Sc (not part of the XRF package used on the magnetic concentrate but showing some association with the axis of the mineralisation) and physical (visible and magnetic) examination of the soil may be used to detect concentrations of magnetite under the colluvium.

TABLE 4
MAGNETITE CONCENTRATES

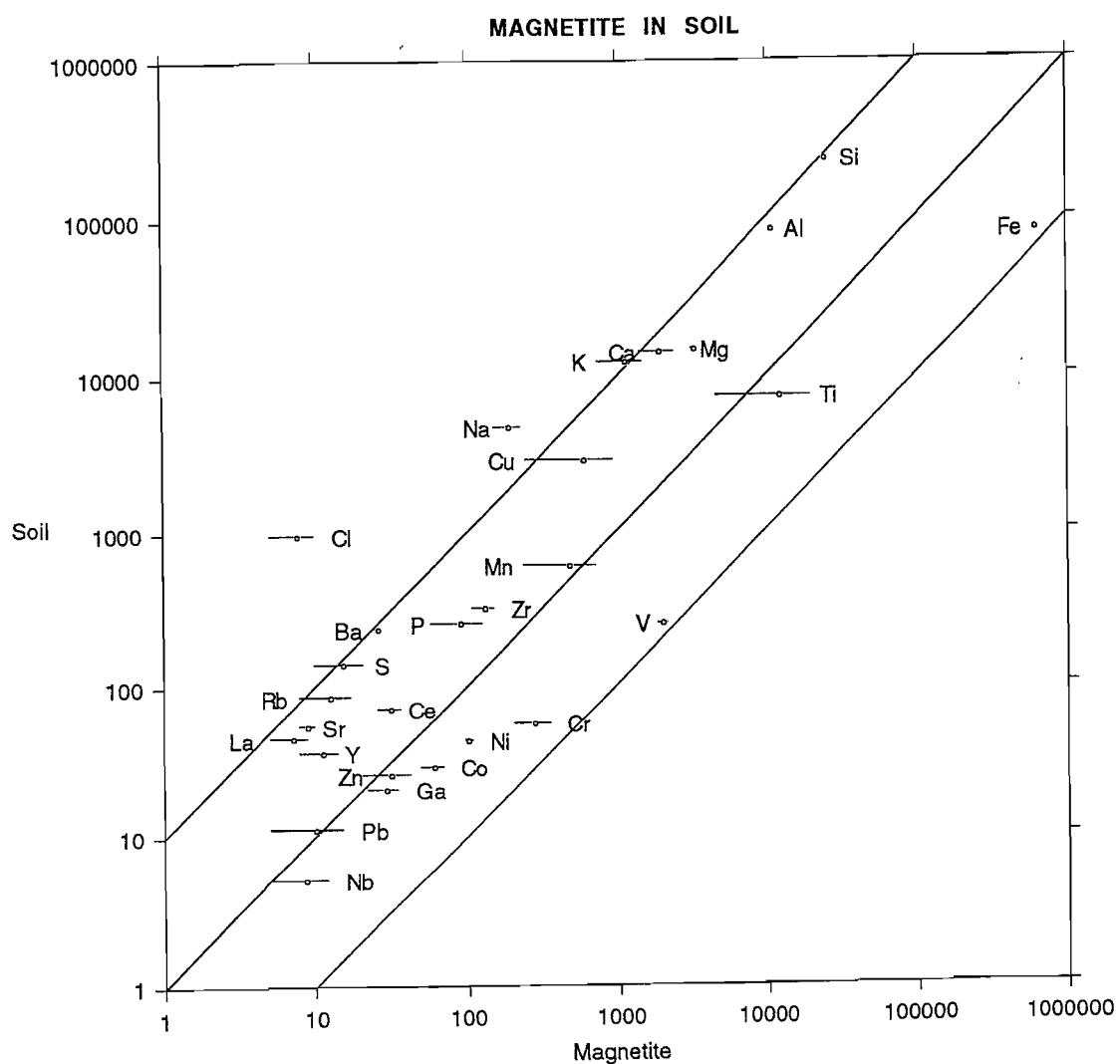| Sample	LE-18	LE-30	Units
SiO2	5.3	5.34	%
Al2O3	2.13	1.98	%
Fe2O3	88.95	87.56	%
MnO	0.03	0.094	%
MgO	0.53	0.57	%
CaO	0.34	0.2	%
Na2O	0.02	0.03	%
K2O	0.09	0.18	%
TiO2	0.77	3.32	%
P2O5	0.028	0.013	%
Ba	27	24	ppm
Ce	25	36	ppm
Cl	0	10	ppm
Cr	202	352	ppm
Co	67	48	ppm
Cu	946	245	ppm
Ga	22	35	ppm
La	4	9	ppm
Ni	94	107	ppm
Nb	12	3	ppm
Pb	2	15	ppm
Rb	8	17	ppm
S	10	20	ppm
Sr	10	8	ppm
V	2155	1880	ppm
Y	8	14	ppm
Zn	20	41	ppm
Zr	108	147	ppm

Figure 15. Log-log plot of mean soil elemental abundances against ranges occurring in soil magnetic concentrate.

8   SUMMARY AND CONCLUSIONS

8.1   Regolith-landforms

Regional

Regolith-landforms, revealed by study of Landsat TM imagery and selected field traverses, shows low hills of quartzites and quartz veins in the south which have shed abundant quartz-rich colluvial material onto pediments. These are now mantled by acid red earths and a lag of ferruginous gravel, lithic fragments and quartz which largely obscures a basement of Proterozoic rocks. Near Cabbage Tree Creek, where erosion has been active, this cover is thin and ferruginous lithosols and a few outcrops of the basement occur on the flanks of small gullies; colluvial materials occur on the crests of the interfluves. The north-west of the area is dominated by colluvial-alluvial materials and blankets of black clay soil.

Local

The Little Eva Cu Prospect lies near the confluence of two braided river channels that drain the Knapdale quartzites. The prospect is sited on a gently inclined, undulating pediment, covered by a thin veneer of colluvium and carbonate-free ferruginous lithosols. There appear to be two minor subdivisions of the colluvium. To the north there is a red-brown lithosol, covered by a lag of locally derived, subangular clasts of quartz and exogenous pebbles and cobbles of quartzite. This lacks the abundant magnetite clasts common in soils overlying the basement. To the south is a red-brown, acid lithosol mantled by a polymictic lag of subangular pebbles of quartz, numerous nodules of magnetite and cobbles of exogenous quartzite. This is interspersed by a ribbed pattern of depressions filled with brown, cracking 'gilgai' soils[3] with no lag.

To the north is a blanket of alluvium exposed in Cabbage Tree Creek, which has graded to basement. The alluvium has a thin basal conglomerate. The south-east margin of the alluvium is linear and probably marks a possibly fault-controlled scarp. Between colluvium and alluvium, small streams in gullies have eroded the colluvium, and weathered basement, rich in calcrete, is either exposed or more commonly, mantled by thin lithosols, generally also rich in carbonate.

Field relationships suggest that the colluvium and gilgai structures in the south-east of the mapped area represent the last stages of dismantling of the colluvium and this is supported by the relative abundance of basement-derived magnetite clasts in the lag on this colluvium. The northern colluvium probably represents a slightly higher unit, an hypothesis apparently supported by apparent but subtle height differences shown by the air photographs.

It is difficult to determine the weathering history without artificial sectional exposure of the regolith, so conclusions must be preliminary. It appears that there was early weathering and erosion of a landscape of Proterozoic basement rocks to gently inclined slopes with low hills and ridges of resistant materials. Weathering of this surface developed abundant calcrete in calcium-rich (mafic) materials. Deflation of the surface left a lag of partly rounded magnetite clasts and angular quartz fragments, both locally derived, on a lithosol.

---

[3]This pattern of ribbed, linear features seems related to gilgai forms, which are common in eastern Australia (Hubble *et al.*, 1983), where similar, ribbed patterns have been reported (also Thompson and Beckman, 1982). Gilgai is a generic term for soil micro-relief patterns, typical of clayey soils with a high coefficient of expansion with seasonal changes in water content. Their origin is controversial (Ollier, 1966; Paton, 1974; Beckman *et al.*, 1981; Thompson and Beckman, 1982) but swelling and shrinking of clay subsoils are important in the development of gilgai. A combination of crack filling and differential wetting (via cracks) controlled by water movement down gentle slopes are thought to be significant processes in the development of linear gilgai.

Sheetwash and minor stream systems have brought in resistant quartz and quartzite clasts from the low hills to the south and have left an extensive but thin blanket of colluvium and minor alluvium over the weathered metamorphics. Later erosion, possibly related to re-grading of major fluvial channels, has etched into this inclined colluvial pediment, locally dismantling the colluvial blanket near the streams, re-exposing the basement and depositing alluvial detritus along the flanks of major channels. Where dismantling of the colluvium was almost complete, the low-gradient drainage pattern closely approximated the original eroded surface of the Proterozoic basement. This dismantling gave rise to patterned 'gilgai' ground, developing smectitic soils from re-weathering of the basement under conditions of restricted water flow and leaving a lag of magnetite clasts from the basement mixed with exogenous quartzite cobbles from the colluvium-alluvium.

8.2 Soils

Eroded basement
Soils, formed on the eroded basement, are immature and contain much of the relatively fresh metamorphic rock (granofels) and derived mineral matter of this basement and are rich in carbonates. Weathering is restricted to turbidity in plagioclase particles and very minor oxidation and hydration of magnetite. The grain size distributions of these soils are bimodal, with a poorly-developed coarse and a well-developed and abundant fine fraction.

Colluvium
The colluvium has a skewed particle size distribution and consists largely of fine material. Soil particles are polymictic and indicate a variety of provenances (granite, quartzite, several metamorphic types and mafic volcanic terrains). Many of the weatherable fragments have stained rims and internal cracks are filled with Fe oxides. Magnetite fragments show more extensive alteration to kenomagnetite than those from the erosional regime. There seems to be adequate evidence for derivation of the exogenous colluvial-alluvial detritus from distant previously weathered terrains. Some of the weathering may have developed subsequently, within the colluvium.

Alluvium
Polymictic particles and a wide variety in the degree of particle rounding characterise the alluvium, indicating derivation from a variety of terrains, both proximal and distal. The bell-shaped particle size distribution and its mode are indicative of hydraulic sorting in a relatively slow flowing fluvial or overbank system.

Fine fraction
The fine (<75 μm) fractions of all these soils is dominated by silt-sized particles of quartz, and finer clays (kaolinite and smectite), with minor feldspar, amphibole, calcite, hematite, magnetite and mica. Carbonates form a major component in soils from the erosional regime.

Importance of bioturbation
Bioturbation by soil mesofauna (worms, insects and other small animals) plays an active role in mixing soils in near surface horizons (Butt and Zeegers, 1992). Williams (1968) calculated that erosion of termite mounds in northern Australia contributes 30 mm to the topsoil every 1000 years.

Termitaria are restricted to areas mantled by colluvium, where they are an important feature of the landscape. Here, although some of the fine fraction would be expected to have been remotely derived, a significant portion of fines would be expected to have been moved upwards, from the weathered basement, and mixed with the exogenous component of the soil. It is probably this bioturbated fine material, consisting of clays and Fe oxyhydroxides and some coarser particles,

that carries the geochemical signal from the basement into the colluvium, although there may have been some hydromorphic dispersion of Cu and Au. It would be extremely difficult to tell which mechanism had been dominant. Details of size fraction analysis and chemical analyses of a sample of a termitarium from the colluvial area are provided in Appendix 8.

8.3   Geochemistry

Pathfinder elements

Indicator elements for Little Eva mineralisation are restricted to Cu and Au. Both work well in soils on the erosional regime for both soil fractions, although the strength of the signal is five fold in the fine (<75 µm) fraction. Copper, in both size fractions, also shows a muted anomaly in the colluvium which closely follows the Cu distribution in bedrock. Gold also shows this trend but only in the fine fraction,. Although W may be useful, a more sensitive analytical method is required to assess it properly. No other elements appear to be directly associated with the mineralisation.

Magnetite and associated elements

Magnetite is, in part, associated with the mineralisation. Thus, Fe, V and Co may be used to detect magnetite-rich stratigraphy. A ground magnetic survey would be expected to be equally effective.

8.4   Implications for exploration

i)   Regolith mapping is an essential precursor to planning of any surficial geochemical survey and to interpreting the results.

ii)   The ferruginous nodules, contributing to soil and lag at Little Eva consist of partly weathered primary magnetite and should not be confused with lateritic nodules and pisoliths.

iii)   Bioturbation by ants and termites may have had a role in transporting geochemical signals through a thin colluvial mantle, although hydromorphic dispersion could also have been involved.

iv)   A thin colluvial mantle provides little barrier to the dispersion of Cu and Au from basement to soil, provided that the fine fraction is used. The alluvium was not penetrated.

V)   Proper attention needs to be paid to muted anomalies in covered areas (possibly by use of logarithmic transforms).

vi)   Copper and Au are indicators for mineralisation at Little Eva.

vii)   If the apparent association of magnetite with mineralisation is confirmed, analysis for Fe, V and Co may be used to detect magnetite-rich stratigraphy. Ground magnetics would be expected to be equally effective.

viii)   Sampling should be avoided in areas where cattle gather and supplementary feeds may have been provided. Contamination by Zn, Cu, Se, Mo, alkalis, P, REEs, U, Ca and S may be expected. Contamination by Zn and P were particularly apparent in this case study.

8.5 Recommendations for further research

i) Exploration of the clay fraction (<2 µm).

ii) Analysis of the soils for W by a sensitive method.

iii) Further regolith-landform mapping on a regional scale.

9 ACKNOWLEDGMENTS

10 REFERENCES

Anand, R.R. and Gilkes, R.J. 1984. Mineralogical and chemical properties of weathered magnetite grains from lateritic saprolite. Journal of Soil Science 35. 559-567.

Beckman, G.G., Thompson, C.H. and Richards. 1981. Relationships of soil layers below gilgai in black earths. In J.W. McGarity, E.H. Hoult and H.B. So (Eds). The properties and utilisation of cracking clay soils. Reviews in Rural Science 5. 64-72.

Blake, D.H. 1987. Geology of the Mount Isa Inlier and environs, Queensland and Northern Territory. Dept of Resources and Energy Bureau of Mineral Resources, Geology and Geophysics Bulletin 225.83 pp.

Edwards, R.G. 1978. Little Eva Cu Prospect, Northwest Queensland M.F. 3072, M.25 5670, 5694, 5695, 5699, Exploration 78. CRA Exploration Internal Report No 9599.

Gozzard, J.R., Munday, T.J., Hunter, W.M. and Gabell, A.R. 1992. An evaluation of SPOT panchromatic imagery as an aid to regolith-landform mapping in the Ora Banda area, Eastern Goldfields Province, WA. CSIRO Division of Exploration Geoscience Restricted Report 233R.

Hubble, G.D., Isbell, R.F. and Northcote, K.H. 1983. Features of Australian soils. In Soils: an Australian viewpoint, Division of Soils, CSIRO. (CSIRO: Melbourne/Academic Press: London. 28-33.

Leeder, R.M. 1982. Sedimentology: Process and product. George Allen and Unwin, London. 344 pp.

Morris, R.C. 1985. Genesis of iron ore in banded iron-formation by supergene and supergene-metamorphic processes - a conceptual model. In K.H. Wolf (Ed). Handbook of strata-bound and stratiform ore deposits. Regional studies and specific deposits. Vol 13. Elsevier. 73-235 (CHECK RIGHT ONE!).

Norrish, K. and Hutton, J.T. 1969. An accurate X-ray spectrographic method for the analysis of a wide range of geological samples. Geochimica et Cosmochimica Acta. 33. 431-435.

Ollier, C.D. 1966. Desert gilgai. Nature No 5062. 581-583.

Paton, T.R. 1974. Origin and terminology for gilgai in Australia. Geoderma, 11. 221-242.

Thompson, C.H. and Beckman, G.G. 1982. Gilgai in Australian black earths and some of its effects on plants. Trop. Agric (Trinidad) 59 No 2. 149-155.

Williams, M.A.J. 1968. Termites and soil development near Brocks Creek, Northern Territory. Australian Journal of Science. 31. 153-154.

Wilson, I.H., Little, M.R. and Robertson, A. 1976. Quamby map sheet. Australia 1:100 000 Geological Series. Bureau of Mineral Resources Geology and Geophysics.